MULTI-PROXY RECONSTUCTION OF A ~1.3 Ma FRESHWATER WETLAND. OLDUVAI GORGE, TANZANIA

by

Kevin R. Garrett

A thesis submitted to the

Graduate School-New Brunswick

Rutgers, The State University of New Jersey

In partial fulfillment of the requirements

For the degree of

Master of Science

Graduate Program in Geological Sciences

written under the direction of

Dr. Gail M. Ashley

And approved by

_____

_____

_____

New Brunswick, New Jersey

January 2017

ABSTRACT OF THE THESIS

Multi-proxy Reconstruction of a ~1.3 Ma Freshwater Wetland, Olduvai Gorge, Tanzania

by KEVIN GARRETT

Thesis Director:
Gail M. Ashley

Reconstruction of paleoenvironmental and paleoclimatic conditions is an important part of the interpretation of geological records, especially for deposits associated with fossils or cultural remains. This study presents a high resolution reconstruction of a ~1.3 Ma paleowetland in Olduvai Gorge, Tanzania, based on facies architecture, composition, clay mineralogy, grain size, stable isotopes, and biological remains (diatoms and phytoliths). Outcrops of a siliceous silt/carbonate packet were mapped over a distance of 1.5 km; stratigraphy was exposed in ten 1-3 m deep trenches. Five facies are identified and form the stratotype: sandy silt, siliceous earthy silt, carbonate, waxy sandy silt, and brown silty clay. The environment of deposition was a wetland with localized distributary channels formed at the distal end of a fluvial plain and margin of a saline-alkaline playa lake. The sequence starts with a sandy silt deposited as terminal splay delta or playa lake margin sands. The wetland sequence overlies this sandy silt and consists of a siliceous earthy silt (and local brown silty clay deposits) and an overlying carbonate. Phytoliths and diatoms record a biologically rich environment. The carbonate contains freshwater fossils and has a stable isotope signature reflecting meteoric source water. The sequence is capped with waxy sandy silts deposited as the playa lake expanded and drowned the wetland. The sequence records the effects of a

rising water table related to more positive water budget (dry to wet portion of a Milankovitch precession cycle). This wetland was a persistent source of freshwater on the landscape for thousands of years. It would have provided a useful source of both food and water for the two species of hominin found in Olduvai at this time – *Homo erectus* and *Paranthropus boisei.*

ACKNOWLEDGEMENTS

I would like to thank those who funded my work and allowed this project to be carried out, including the Geological Society of America, The National Association of Black Geologists, The Society for Sedimentary Geology, Rutgers New Brunswick Graduate School, and the Rutgers Department of Earth and Planetary Sciences.

Thanks to COSTECH and the Ngorongoro Conservation Association for permitting and allowing me to work in Olduvai. Also to TOPPP, most specifically Manuel Dominguez-Rodrigo and A.Z.T. Mabulla. Thanks to January Qwaray for his help in the field.

I appreciate the contributions made by R. Bernhart Owen for diatom analysis and Doris Barboni for phytolith analysis. Also, I am grateful to David Davis, Daniel Deocampo, and Emily Beverly for clay mineral analysis (Dept. of Geosciences, Georgia State University) and Ben Horton and Tina Dura for access to the Malvern grain size analyzer (Dept. of Marine and Coastal Sciences, Rutgers University). My sincere thanks to Jim Wright and Rick Mortlock for their help with all things carbonates and beyond.

Thanks to my Advisor Gail M. Ashley for all of her help every step of the way. Thanks also to my committee, John Reinfelder and Craig Feibel. Thanks to Carl Swisher, Chris Johnson, Gabe Gallegos, and everyone else at EPS for all of your help along the way. Thanks to my mom, Claire and sister, Nicole for their continued love and support. Thanks finally to my father, who continues to be my inspiration daily. I thank God that I'm finished, and I thank god that I'm finished.

TABLE OF CONTENTS

LIST OF TABLES

LIST OF FIGURES

LIST OF APPENDICES

INTRODUCTION

Wetlands are found on all continents and cover 4-6 per cent of the land surface (Tooth and McCarthy, 2007). Often supporting diverse and endemic species, wetlands are unique areas on the landscape (Springer and Stevens, 2008). High productivity and availability of water makes wetlands attractive to humans, and they thus have been an important resource for human habitation through time (Tooth and McCarthy, 2007; Nicholas, 2013; Cuthbert and Ashley, 2014). There is a growing body of literature on fossil freshwater deposits in the geologic record, especially those deposited in arid climates (Liutkus and Ashley, 2003; Owen et al., 2009; Pigati et al., 2014). The study of fossil wetlands in arid settings is particularly important for East African early human habitats, because fresh water was likely scarce (Cuthbert and Ashley, 2014). A number of factors complicate the study of fossil wetlands. Paleowetland deposits are typically found in low topographical areas but may be difficult to recognize because of their relatively small size. In addition, they may also be overprinted by diagenesis or eroded by the expansion and contraction of nearby lakes (Quade et al., 1995; Deocampo, 2002a; Pigati et al., 2014). Wetlands are also difficult to differentiate from lacustrine sediments, being fine grained and often containing similar fossil fauna (Quade et al., 1995; Alonso-Zarza and Wright, 2010). Despite their elusiveness they can be important in reconstructions of environment and the hydrologic budget (Quade et al., 1995; Rech et al., 2002; Alonso-Zarza, 2003; Quade et al., 2008).

Olduvai Gorge is a small basin on the margin of the Gregory Rift in the East African Rift System (EARS) (Figs. 1, 2). This endorheic basin is flanked on the east and

south by the Ngorongoro Volcanic Complex and the Serengeti to the north and east. The area gained fame in the 1960s when several landmark hominin sites were described by Mary and Louis Leakey (Leakey, 1965; Leakey, 1971; Leakey, 1979). Among its important contributions to the paleoanthropological record are the first descriptions of two species: *Paranthropus boisei* and *Homo habilis* (Leakey, 1971). These discoveries were critical for scientific understanding of early human evolution, helping to contest the notion that hominins evolved in East Asia (Etler, 1996) and helped prove that early human origins lie in Africa. The Pleistocene hominin sites at Olduvai are archived in deposits of a ~50 km diameter basin (Figs. 2, 3) A playa lake occupied the center of the basin from 2-1 million years ago. The close association of the stone tools to paleo Lake Olduvai suggested that they were lake margin sites, and that a lake assumed to be fresh was attracting hominin and animal activity (Leakey, 1971; Blumenschine and Peters, 1998). Later geochemical analysis showed the lake was alkaline and saline, and not a potential source of drinking water for hominins (Hay and Kyser, 2001).

Many studies of Olduvai Gorge have focused on the interaction of climate and the geologic record (Magill et al., 2013b; Ashley et al., 2014a; Ashley et al., 2014b; Beverly et al., 2014). The importance of lake deposit cyclicity has been recognized since Europeans first explored the East African Rift (Selley, 1997), but only recently has it been discerned that precession cycles were the controlling factor on East African lake size through most of the Pleistocene (Trauth et al., 2005; Deino et al., 2006; Kingston and Hill, 2006; Ashley, 2007). Episodic volcanism from the nearby Ngorongoro Volcanic Complex generated tephra deposits that are intercalated with fossil-rich deposits. Precise dating of these tuffs allows for high detail reconstructions of past environment and

climate as well as the fossil record. Combined geologic and paleoanthropological studies in the Gorge have aimed at reconstructions of various scales, from individual sites (Dominguez-Rodrigo et al., 2009; Bunn et al., 2010) to areas on the landscape to broad basin-wide interpretation (Hay, 1976; Deocampo et al., 2002; Albert and Bamford, 2012; Magill et al., 2016). Such large-scale studies provide context of what environmental factors may have influenced early human evolution (Potts, 2013).

Olduvai Gorge consists of two river gorges (the Main Gorge and the Side Gorge) that join as the Olduvai River flows eastward towards the Obalbal Depression (Fig. 3). One of the earliest paleoanthropological sites in the Side Gorge is BK (Bell's Korongo). This site was first intensively excavated by Mary and Louis Leakey in 1963, and was reopened by Manuel Dominguez-Rodrigo and Audax Mabulla in 2006 (Leakey, 1971; Dominguez-Rodrigo et al., 2013). A *Paranthropus boisei* partial skeleton was found in the most recent excavation. A *H. erectus* ulna was found at a stratigraphically equivalent site further east in the Side Gorge (site SC) – excavated by Mary Leakey. Two separate hominin genera were living in or at least visiting the Olduvai Basin during this time period, termed Upper Bed II. It is the last appearance for *P. boisei* in the region, and thus a potentially important time of change in the local hominin species (Dominguez-Rodrigo et al., 2013). Since East African climate has become increasingly arid for the past several million years, access to fresh water must have become increasingly difficult through that time (Cerling et al., 1993; Potts, 1994; deMenocal, 1995).

During recent paleoanthropological excavations at BK a distinctive deposit ~1m thick was recognized extending over 1 km through the basin, outcropping on both the north and the south faces of the Side Gorge. However, no detailed mapping, trenching, or

analysis of the siliceous earthy silt had been done. This unit consisted of a carbonate overlying a siliceous earthy deposit. Preliminary investigation of isotopic signatures and biological remains of the carbonate indicated that this was a freshwater deposit (Ashley et al., 2014b). Little was known about the paleoenvironment, but the facies association suggested this was a freshwater environment fringing a deltaic system on the margin of a lake.

Objectives

The objectives of this study are to (1) describe, characterize, and interpret the siliceous earthy deposit and limestone beds in terms of depositional environment, (2) create a facies model for the sedimentary package and surrounding sediments, and (3) interpret the records in terms of the regional paleoclimate record. This is to be achieved using field descriptions of sedimentology and stratigraphy, grain size analyses, mineralogy, isotope geochemistry, and biological analyses. This deposit is physically associated with at least three archaeological sites with evidence of hominins (BK, SC and SHK). This study will be one of the few geological studies to focus on Upper Bed II in Olduvai, a period of time that has not been a prominent area of focus of detailed sedimentological research.

BACKGROUND

Geologic Setting

Olduvai Gorge is a sedimentary basin located on the western margin of the Gregory Rift in the East African Rift System (EARS), Tanzania (Fig. 1). It is in the area

of the system called the Northern Tanzanian Divergence, where the EARS splits into two separate rifts (Foster et al., 1997; Dawson, 2008; Le Gall et al., 2008). The Gorge sits between the Ngorongoro Volcanic Complex (NCV) to the east and south and Pre-Cambrian metamorphic basement to the north and west (Fig. 2). While volcanism began in the NVC around 4 Ma, the flood basalts ~2 Ma are considered the basal unit of the Olduvai sequence (Hay, 1976; Deino, 2012) (Fig. 4). As a result of explosive volcanism in the NVC, tephra deposits intercalate with sedimentary deposits in the sedimentary sequence. Tephra deposits in Olduvai can be traced and correlated through the basin (Hay, 1976). Tuffs at Olduvai are well described in terms of their composition and their geochemistry (McHenry, 2005; McHenry et al., 2008; McHenry et al., 2016). These tuffs can be dated precisely, principally by $^{40}Ar/^{39}Ar$ (Deino, 2012). Studies of sedimentary infill between tuffs allow for high resolution reconstructions of paleoenvironments and enables correlation of these time slices throughout the Gorge (Liutkus and Ashley, 2003; Ashley, 2007; Copeland, 2007; Kovarovic et al., 2013; Beverly et al., 2014).

During the Pleistocene, Olduvai was an interior drained terminal basin, where ephemeral low gradient streams drained into an alkaline, saline playa lake. The lake ranged in size from ~10 km in diameter to ~under 5 km depending on stages in precession cycles (Hay, 1976; Ashley and Hay, 2002)(Fig. 3). The basin contains a ~100 m thick Pleistocene sequence of intercalated volcanic and sedimentary rocks, spanning from about 2-1 Ma. This sequence is dominated by fluvial, alluvial, and lacustrine deposits of volcaniclastic composition. Episodic rift-related normal faulting has shifted the center of the basin eastward over time, resulting in its current low point Obalbal Depression, a fault bounded graben. The Obalbal Depression is the terminus of an

ephemeral fluvial system beginning at Lake Masek at the east margin of the Serengeti Plain, ~50 km to the west. This drainage system incised the modern Gorge in the late Pleistocene (~20 Ka) Fig. 3). The down-cutting was likely triggered by rift related tectonics (Hay, 1976).

Detrital sediments in the Gorge derive primarily from three sources: 1. The volcanic highlands to the east and south, 2. Pre-Cambrian metamorphic bedrock to the north and west and 3. Eolian and fluvial sediments from the Serengeti to the northwest (Ashley and Hay, 2002). Chemical sediments are dominantly lacustrine and include authigenic clays such as illite and smectite (Hover and Ashley, 2003). Carbonate deposits are common, but localized in both time and space. They occur mainly in basin infill (Beds I and II) (Ashley et al., 2014b).

The stratigraphic sequence at Olduvai Gorge, which was initially named by Reck (1951) and later defined by (Hay, 1976), includes 5 Beds. They range from Bed 1 to the Bed 5 (Ndutu/Naisiusiu Beds), with the latter being Holocene in age and limited in extent. These beds can be traced across the Gorge. The stratigraphic delineation of Bed II (1.8-1.2 Ma) has been somewhat equivocal in scientific literature (Kovarovic et al., 2013). It is commonly divided into Lower, Middle, and Upper intervals (Leakey, 1971) with some authors omitting Middle Bed II (Hay, 1976) (Fig 4). Previous geological studies have largely focused on Uppermost Bed I and Lowermost Bed II – this time slice (1.9-1.75 Ma) can be well traced through much of the Gorge. Upper Bed II is not as well correlated through the basin because its tuffs are not as easily identifiable (McHenry et al., 2016). This study examines in Uppermost Bed II, above Tuff IID (~1.34 Ma) (Dominguez-Rodrigo et al., 2013) (Fig. 4).

Climate

After a climatic optimum in the mid-Miocene, the world has broadly seen a drying and cooling trend over the past ~8 Ma (Cerling et al., 1993). The literature is equivocal in regards to the specific triggers of this drying, but potential causes have been suggested. The uplift of the Tibetan Plateau has long been thought of as a strong contributing factor, and could have contributed to global aridity via an increase in silicate weathering, the net result of which is a drawdown of CO2 (Rea et al., 1998). With this drawdown of CO2 comes a decrease in global air temperature. Cold air is less capable of holding moisture than warm air, thus there was a global increase in aridity (Rea et al., 1998). Still, the literature remains ambivalent as to when exactly the Tibetan Plateau achieved its current height (Molnar et al., 1993; Miao et al., 2012). Regardless of cause, this increase in aridity around 8 Ma is marked by a near simultaneous rise of grasslands around the world (Cerling et al., 1993). The sudden success of C4 plants was initially thought to be related to a late Miocene drop in atmospheric CO2 levels, as C4 plants are more successful in low-CO2 environments (Cerling et al., 1993). Subsequent analysis showed that a critical threshold for C4 success had previously been crossed in the Miocene, and thus some other factor must be responsible (Pagani et al., 1999). There are multiple signs of this aridity: it is marked by increased eolian dust input in the Atlantic and Pacific Oceans (deMenocal, 1995; Rea et al., 1998) and a near simultaneous rise of C4 grasslands on three continents: Asia, Africa, and North America from soil carbonates (Cerling et al., 1993). These represent the earliest C4 grassland biomes in the geologic record.

The rise of the grassland biome had profound ecological implications. Faunal turnover was pervasive – biodiversity of large herbivores drops precipitously, grazing herbivores are more successful, and different communities of rodents take hold. Such effects occur in several continents (Cerling et al., 1997). In Asia, increasing aridity has been shown to correlate with a marked increase of the strength of the monsoon (Quade et al., 1989). The savannah biome has long been thought of as an important factor relating to the development of hominin bipedalism (Dart, 1925), and indeed genetic and fossil evidence suggests hominins developed bipedalism around 6-7 Ma (Zollikofer et al., 2005; Richmond and Jungers, 2008). The "Savannah hypothesis" broadly states that bipedalism gave hominins distinct advantages in grasslands over forests. Bipedalism grants ability to see farther, more efficient locomotion to travel further distances, and frees the hands to be able to carry objects to remote locations.

Further drying in the late Pliocene (~4 Ma) has been attributed to major oceanographic changes. The closing of the Panama Isthmus and the closing of the Indonesian Seaway (Rea et al., 1998; Cane and Molnar, 2001) would have had profound consequences for ocean circulation and are thought to have contributed both to global aridity and East African aridity. These oceanographic changes are also thought to have led to the onset of Northern Hemisphere Glaciation or the establishment of a permanent ice sheet in the Northern Hemisphere (Rea et al., 1998). Local aridification in East Africa may have been enhanced by orographic effects. Models have shown that major uplift in the Olduvai region from 5 to 2 Ma would have led to an overall increase in aridity (Sommerfeld et al., 2014; Jung et al., 2015). Global climate has grown increasingly arid over the past 2 Ma (deMenocal, 1995). This is potentially reflected at Olduvai in both

mammal and plant ecology changes (Plummer and Bishop, 1994; Fernandez-Jalvo et al., 1998; Kovarovic et al., 2013). From Bed I through Lowermost Bed II Olduvai changed from a woodland environment to a more open environment with patches of woodland (Copeland, 2007). However, local climates often fail to correlate directly with global climate over long time scales. The ecological changes at Olduvai may have been a result of less available fresh water due to tectonic changes in the Gorge. As a result of normal faulting, the depocenter of the Gorge shifted eastward through time. The landscape changed from a lacustrine environment to an ephemeral fluvial system. The lack of permanent fresh water may have had significant ecological impliucations, independent of global scale climate change. Upper Bed II coincides with the last appearance of the genus *Paranthropus* in East Africa (Dominguez-Rodrigo et al., 2013). However, *Homo* was successful in Africa and Eurasia during this timeframe.

Milankovitch cyclicity has long been recognized as a driver of global climate (Ruddiman, 2000). During much of the Pleistocene, glacial-interglacial cycles were driven by obliquity (Ruddiman et al., 1988). During this timeframe the tropics were operating independently of higher latitudes and were forced by precession cycles. Precession cycles affected the strength of monsoons and thus rainfall totals in tropical regions throughout the world (Maslin et al., 2014). The variability of rainfall over 23 kyr scales caused periodic swelling of the various basin lakes in the EARS (Deino et al., 2006; Ashley, 2007). Precession-driven climate fluctuations had an effect on local flora and fauna. The availability of freshwater allowed for different plant communities, which attracted vertebrate life (Copeland, 2007; Barboni, 2014). Hominins focused their activities to be near these plant and animal rich environments (Ashley et al., 2009).

Paleoenvironmental Setting

Interdisciplinary studies have recreated the paleoenvironment of Olduvai Gorge through analyses of sedimentology, pollen, geochemistry, diatoms, phytoliths, biomarkers, and vertebrate fossils (Bonnefille, 1984; Plummer and Bishop, 1994; Bamford, 2005; Barboni et al., 2010; Albert and Bamford, 2012; Magill et al., 2013a). The Pleistocene climate of Olduvai Gorge ranged from arid to semi-arid, similar to its modern climate. During the Pleistocene mean annual precipitation was calculated to range from 250 to about 750 mm/yr, compared to a modern average of 550 mm/yr (Magill et al., 2013b), with rainfall being controlled by precession cycles (Ashley, 2007). The Ngorongoro Highlands to the east create a rain shadow, blocking easterly moving moisture from the Indian Ocean. The resultant precipitation on the Highlands moved into Olduvai Basin via both fluvial and groundwater systems, ultimately reaching paleo Lake Olduvai at the center. A playa lake, paleo Lake Olduvai changed in size seasonally but also changed maximum size via longer term precessional cycling (Ashley, 2007).

Groundwater-fed wetlands occurred at the bottom of the basin margin slope (Ashley et al., 2014b). The presence of fresh water in the Gorge allowed for a variety of "wet" microenvironments and wide range of plant life (Barboni, 2014). The percentage of woody cover was also influenced by precession cycles (Magill et al., 2013a). During the Pleistocene, Olduvai was either a closed or partially closed woodland environment (Fernandez-Jalvo et al., 1998; Copeland, 2007). The density of woody plant cover fluctuated with precession cycles. Increased rainfall during precession maxima led to larger shrubs and trees, providing shaded environments that were focal points for hominin activity (Ashley et al., 2009; Magill et al., 2016).

A combination of increased aridity and tectonic changes in basin shape led to the shrinking of paleo Lake Olduvai from Bed I to Upper Bed II times (Stollhofen and Stanistreet, 2012). Increased aridity across the African continent during the Pleistocene is not only reflected across in dust flux delivery to the ocean (deMenocal, 1995), but is also ecologically expressed at Olduvai. Studies of mammal ecology have suggested that during Bed I times Olduvai was a closed woodland environment that grew progressively more open and arid towards the top of the Bed (Plummer and Bishop, 1994; Fernandez-Jalvo et al., 1998). Average body mass of large mammals shrinks from Lower Bed II to Upper Bed II, and a decrese in the diversity of rodents, carnivores, primates and bovids point to increased aridity during this time frame (Kovarovic et al., 2013).

Freshwater Deposits at Olduvai Gorge

It was originally thought that paleo Lake Olduvai was a freshwater lake because of the abundant evidence of animal life. However, subsequent analysis showed that the lake was saline and alkaline, and not potable for hominins (Hay and Kyser, 2001; Hover and Ashley, 2003; Deocampo et al., 2009). More recent research has focused on various small freshwater deposits in the Gorge, which were initially overlooked by more broad-scale geological studies (Hay, 1976). Freshwater deposits in the Gorge are frequently present in the form of "siliceous earthy clays" which are wetland deposits and are notable for the presence of rhizoliths, diatoms, phytoliths, and other signs of life (Liutkus and Ashley, 2003; Liutkus et al., 2005). These earthy clay deposits commonly alternate with "waxy" lake clays and signify lake transgressions/regressions respectively (Deocampo et al., 2002; Liutkus and Ashley, 2003). A wide range of wetland and spring facies have

been described at Olduvai, including tufa mounds, fault-associated springs, and widespread seeps (Ashley et al., 2014b).

Wetlands are an important part of the climatic history of Olduvai, as their presence is typically indicative of precessional climate cycles (Deocampo et al., 2002; Ashley et al., 2014b). During maxima, paleo Lake Olduvai expanded over the lake margin flats and flooded the wetlands, depositing waxy sandy silts. During waning precession limbs the lake shrank, exposing freshwater-fed springs and seeps. These lush wetlands supported plant and animal life and accumulated earthy clay/silt deposits. Thus, wetlands usually formed during dry periods in precession cycles. Examples of this mode of sedimentation can still be seen today in the endorheic basins of East Africa (Deocampo, 2002a). In Tanzania and Kenya, modern lake-fringing wetlands exist because the lakes have shrunk significantly since their maxima during the African Humid Period ~7,000 years ago (Deocampo, 2002b).

Paleoanthropology

Olduvai Gorge is famous for its rich contributions to the paleoanthropological record, and evidence of occupation of four species of hominin has been found there: *Paranthropus boisei*, *Homo habilis*, *Homo erectus*, and *Homo sapiens*. Two of these species, *P. boisei* and *H. habilis*, were first described at Olduvai (Leakey, 1959; Leakey et al., 1964; Leakey, 1971). During the time interval of the present study, Upper Bed II, at least two hominins frequented Olduvai: *Homo erectus* and *Paranthropus boisei.* The sediments in this study are stratigraphically equivalent to the hominin-bearing archaeological site SC, older than BK, and younger than BK-East (Fig. 5). At BK, a *P.*

boisei partial skeleton was found, and at SC a *H. erectus* ulna (Leakey, 1971; Dominguez-Rodrigo et al., 2013). Developed Oldowan B artifacts were found at both sites (Leakey, 1971). *P. boisei* would soon after become extinct in East Africa.

It has been shown that changes in wet/dry climates altered hominin behavior (Potts, 2013). During dry periods hominins would focus tool-making activity around areas with fresh water (Ashley et al. 2009). Similarly, hominins have been shown to prefer more heavily wooded habitats, which would have been scarce during dry times (Magill et al., 2016). The ability of hominins to move among different landscapes on relatively short timescales may have been important for their success. Recent research in human evolution has shown that variable climates may have played an important role in hominin speciation (Potts, 2013).

METHODS

Field Methods

Previous investigation and tracing of the siliceous-carbonate sedimentary sequence was carried out by Ashley et al. (2014b). However, there was no detailed mapping or trenching of the siliceous earthy silt. Fieldwork was performed in June and July, 2015. In this study, the deposits were physically traced over 1.5 km in outcrops on the north and south walls of the Side Gorge (Figs. 5, 6). Location of each trench was determined using a handheld Garmin GPS (Appendix I). A hand level was used to aid correlation between outcrops. Ten 1 meter wide trenches were excavated with a superpik and shovel. The objective was to expose the siliceous earthy-limestone package and the juxtaposed sedimentary units above and below. Seven trenches were excavated on the

south wall of the Gorge and three on the north (Fig. 6). The siliceous earthy unit was subsampled vertically at 5 cm intervals, or 15 cm if the facies was particularly thick. At trenches where no siliceous earthy sediment was present, the brown silty clay was sampled at 5 cm intervals. At least one representative sample was collected from each distinct sediment unit unless the layer was particularly thick (>50 cm). Each trench was photographed and logged. Scaled drawings were made using a tape measure and observations of bedding, sedimentary structures, fossils, and Munsell colors recorded. Oriented samples of the siliceous deposit were collected at every trench for micromorphological assessment. A tuff was found above the carbonate at Trench BK-KG-10. This tuff (sample BK-KG-1015) was sampled and will be dated using single-crystal $^{39}Ar/^{40}Ar$ dating.

The 126 samples collected were organized into the following five facies based on field observations: siliceous earthy silt, carbonate, sandy silt, waxy sandy silt, and brown silty clay. Isolated samples of a tuff (sample BK-KG-1015) and a fine grained tuffaceous unit (sample BK-KG-806) were also logged

Lab Methods

Grain Size Analysis

Sixty samples were measured for grain size distribution, including samples from each facies except for the carbonate and tuff. Approximately 1g samples were placed in 30% hydrogen peroxide at room temperature for 2 days to oxidize and eliminate the organic fraction. When the reaction was less volatile, the samples were placed in a water bath at 55° C for 2 weeks, refreshing hydrogen peroxide daily. The samples were loaded

into a MALVERN instrument using Mastersizer 3000 technology. The samples were analyzed in the Sedimentology Laboratory, Dept. of Marine and Coastal Sciences, Rutgers-NB (Benjamin Horton, Director). Raw data are summarized in Appendix II, A suite of subsamples representing the coarser facies were selected to determine sand/mud percentages. This was done to provide an independent check on the Malvern data.

Carbon and Oxygen Stable Isotope Analysis

The twenty carbonate samples collected were subsampled and analyzed using a Micromass Optima mass spectrometer with attached multi-prep device at the Dept. of Earth and Planetary Science, Rutgers-NB, Stable Isotope Laboratory (James Wright, Director). The samples were powdered, some by using a drill but most with a mortar and pestle. Approximately 100 µg of powdered sample was placed in 100% phosphoric acid for 10 minutes at 90°C. The evolved CO_2 was captured in a liquid nitrogen cold finger. Reported ratios are relative to the Vienna-Pee Dee Belemnite ($\delta^{13}C$ and $\delta^{18}O_{VPDB}$) in standard delta notation parts per thousand (per mille, ‰). Data are summarized in Appendix III.

XRD Analysis

Clay Mineralogy

Clay Mineralogy analysis was performed by David Davis at Dept. of Geosciences, Georgia State University and analyzed in their Environmental Research Lab. (D.M. Deocampo, Director). In accordance with procedures detailed in Deocampo et al. (2010), 100 g samples were soaked in 200 ml of distilled-deionized water along with

several drops of sodium hexa-metaphosphate, a disaggregate. The samples were centrifuged in the manner of Jackson (1969) stepwise at higher speeds to a maximum of 40,000 rpm to isolate the <.01 μm fraction. The 2-0.01 μm fraction contains some non-clay minerals, such as fragments of diatoms and shards of volcanic glass, which could bias results (Deocampo, 2004). Measuring the fraction below 0.01 μm ensures that only actual clay minerals are analyzed.

The samples were air-dried and solvated in ethylene glycol from 3 to 45° 2θ. They were analyzed with a Philips PW1710 at 45 kV and 40 mA following Moore and Reynolds (1989). Twenty samples were analyzed, 12 of which were waxy silt samples and 8 of which were from siliceous earthy silt.

Rhizolith Mineralogy

Representative samples of rhizoliths from the siliceous deposit were analyzed in the Environmental Research Lab., Department of Geosciences, Georgia State University, (D.M. Deocampo, Director). Bulk samples were powdered and run through Phillips PW 1710 X-ray diffractomer. Data are summarized in Table 1.

Biological Analyses

Diatom Analysis

Analysis of diatoms in sediment was performed by the Dept. of Geography, Hong Kong Baptist University (R. Bernhart Owen, Director). Samples were prepared by treatment of 10 g of sediments with HCl (33%) in Pyrex beakers for 4 hours to remove carbonates, and then with H_2O_2 (30%) at 70° C to remove organic matter. The H_2O_2 was

refreshed daily until oxidation reaction ceased. Clays were deflocculated using a solution of sodium polyphosphate ($NaPO_3$, 0.1%) at pH 7 and removed by decantation and centrifugation until supernatant was clear. Diatoms were identified on smear slides mounted in Naphrax. Species level identification was carried out by R. Bernhart Owen with light microscopy at 1000x magnification with reference to Gasse (1986). A total of 14 samples were analyzed, two from each of the seven trenches with siliceous earthy sediments. The assemblages were entered into the European Diatom Database (EDDI, http://craticula.ncl.ac.uk/Eddi/jsp/index.jsp) and run through a Least-Weighted Weighted Average (LWWA) transfer function to obtain conductivity estimates.

Phytolith Analysis

The 10 g samples that were prepared by R.B. Owen were sent to Doris Barboni at CEREGE in Aix-Marseille University, France. The samples were described according to international phytolith nomenclature (Madella et al., 2005). Separation of biogenic silica from the mineral fraction and concentration of phytoliths was achieved using ZnBr2 heavy liquid at a specific gravity of 2.30. Residue (including phytoliths) was rinsed and dried before storage in glass vials. To allow rotation of phytoliths during microscope observations, slides were prepared using a small amount of dry residue mixed with benzyl benzoate as a mounting. Slides were observed using a Zeiss Photomicroscope III, at magnification x500 and x1000. Permanent slides were also mounted with Canada Balsam.

Phytolith morphotypes are described and counted separately. Counting is done until a minimum of 200 grass silica short cells is reached. However, for samples that are

clearly dominated by non-grass phytoliths, counting of GSSC's usually reached 100. Data are summarized in Appendix IV.

Thin Sections

Two oriented samples of siliceous sediment sent to Applied Petrographic Services, Inc., impregnated and made into large (50x75 mm) thin sections. Photomicrographs were taken at Rutgers University in plane polarized and cross-polarized light. The samples used for thin section analysis are BK-KG-3 and BK-KG-5.

RESULTS

Facies Descriptions

Stratotype

Trench BK-KG-2 serves as a stratotype for the sedimentary sequence as it contains a typical succession (Fig. 7). The stratatoype sequence is: sandy silt, siliceous earthy silt, carbonate, waxy sandy silt. The exact sedimentary sequence is variable, and no two trenches were identical. On average, the sedimentary sequence has sandy silt at the base and waxy sandy silt at the top, with the siliceous earthy silt and carbonate beds in between. The brown silty clay facies occurs locally and is not present at localities with siliceous earthy silt.

Sandy Silt

The sandy silt is immature, poorly sorted with angular grains and occurs below the siliceous clay-limestone sequence (Figs. 7, 8, Appendix V). It is 32.4% sand, 43.8% silt, and 23.8% clay. Typically pale yellow (5Y 8/2), it is usually a stronger yellow than the siliceous earthy silt (Fig. 9). The presence of mafic sand-sized grains suggests the source rocks were volcanic. The full thickness of the sandy silt was rarely exposed due to time constraints. At Trench BK-KG-1 it was over 50 cm thick and may have been directly overlying Tuff IID (Fig. 7). It was at least 50 cm thick at Trench BK-KG-9, where the bottom of the sandy silt was not exposed (Fig. 7). It occurs at the bottom of Trenches BK-KG-1, BK-KG-2, BK-KG-3, BK-KG-4, BK-KG-5, and BK-KG- 9, and is the second facies at Trench BK-KG-6 (Fig. 7). It is also the uppermost facies at trench BK-KG-6, the only instance in which the sandy silt is found above the siliceous earthy silt-carbonate sequence. This sandy silt (sample BK-KG-613) is much higher in silt percentage than the other samples, but its similar appearance and mineralogy suggests it is part of the same facies.

Siliceous Earthy Silt

"Siliceous Earthy Clay" is a term coined by Hay (1976) to describe the silica-rich yellow to buff colored clayey and silty units which are locally common in Beds I and II. However, the siliceous units described here are mostly sandy clayey silts, so a modified version of Hay's term is used. The siliceous earthy silt ranges from pale yellow (2.5Y 7/3) to white (2.5Y 8/1) and is characterized by abundant white, siliceous rhizoliths (Figs. 9,10, 11). It is on average 32.3% sand, 47.7% silt, and 20.0% clay. Mineralogy analysis

on the rhizoliths shows the most common phases are opal-A (57% of samples, n=7), opal-CT (43%) and Mg-calcite (43%). Other phases present include dolomite, calcite, quartz, and clays (Fig. 15). However, tests of HCl on hand samples rarely showed fizzing, suggesting that calcite may be present in low quantities in these rhizoliths. This comes in contrast to some other siliceous clay deposits described at Olduvai, where carbonate rhizoliths can be common (Liutkus et al., 2005). The rhizoliths at BK are 2-5 mm in diameter and typically about 1 cm in height, although they range from smaller fragments to up over 5 cm at certain trenches (Fig. 10 B,C). They preserve some of the original shape of the plant. They have striations running along their long axis and are isodiametric – they never taper. They are vertically or nearly vertically oriented except in trenches which appear to be disturbed by either slumping or bioturbation. They are regularly spaced and do not express any noteworthy morphology, such as branching, rootlets, or nodules. Other biological remains found in the siliceous clay include phytoliths, diatoms, and sponge spicules. These are described below. Grain size distributions in the siliceous earthy silt show a high percentage of sand due to an abundance of rhizolith fragments (Figs 8, 11).

Carbonate

Carbonate is typically massive and white to occasionally gray in color, varying in texture from soft powdery to a dense nodular micrite. The term “tufa” used in the manner of Ford and Pedley (1996) i.e. a freshwater carbonate precipitated in ambient temperature waters best describes the deposit. It is the only facies found at every trench. The tufa is of variable thickness but can be traced throughout much of the Side Gorge.

Excavation showed that some localities have two carbonate layers, in which instances the uppermost carbonate is part of the traceable, cohesive tufa bed. Carbonate layers range in thickness from occasional 15 cm seams to a 60 cm thick layer. In some instances the siliceous earthy silt/carbonate sequence repeats itself, resulting in two carbonate layers. This is the case at Trenches BK-KG-3, BK-KG-6, and BK-KG-9 (Fig. 7). At BK-KG-9, one carbonate layer at BK-KG-9 was highly localized, being ~4m wide and pinching out to either side. Some samples of carbonate are intercalated with deposits of waxy sandy silt. The percent carbonate is variable from trench to trench, resulting in the variable color. Rare gastropod and diatom fossils are found, but the tufa is notably lacking in preserved fossils compared to the siliceous silt.

Waxy Sandy Silt

Waxy sandy silt is a poorly sorted clay rich facies which when dry has a waxy sheen. The clay is massive, and no sedimentary structures are apparent. It ranges from very dark greyish brown (2.5Y 3/2) to olive (5Y 5/3) and is commonly mottled with black spots. It is dominantly silt, averaging 43.8% silt, 23.8% clay, and 32.4 % sand (Fig. 8, Appendix V). The waxy sandy silt typically has sharp but highly undulatory boundaries. Its thickness ranges from 12 cm to over 30 cm. It is thickest at Trenches BK-KG-2 and BK-KG-3, where it is the topmost facies. At those trenches its full thickness was not exposed. Waxy sandy silt was present at 7 of the 10 Trenches (BK-KG-1, BK-KG-2, BK-KG-3, BK-KG-4, BK-KG-5, BK-KG-6, and BK-KG-10) (Fig. 7). Its sand sized fraction is largely mafic minerals with minor feldspar and quartz. Illite and smectite are both present, with most samples being dominantly illite. Bulk mineralogy indicates

the presence of plagioclase, augite, phillipsite, analcime, calcite, and some zeolite (Figure 15). It appears twice in trenches BK-KG-1 and BK-KG-6, the two most southeasterly trenches (Fig. 7).

Brown Silty Clay

The brown silty clay is present in two trenches (BK-KG-7 and BK-KG-10) and ranges in thickness from about 60 to 75 cm respectively (Fig. 7). It ranges in color from a dark brown to a pale olive (5Y 6/3) or olive (5Y 4/3). The sand fraction consists of quartz, feldspars, and mafic grains. It averages 15.6% sand, 32.0% silt, and 52.3% clay. It is higher in clay content and lower in sand than the waxy sandy silt (Fig. 8). There is a difference in average grain size between the two trenches it is found in. The brown silty clay is 10.0% sand, 29.6% silt, and 60.4% clay in Trench BK-KG-10. Trench BK-KG-7 is coarser, averaging 21.3% sand, 34.5% silt, and 44.2% clay. Illite is the dominant clay mineral present (Figure 15). Bulk mineralogy includes plagioclase, augite, analcime, quartz, and some chabazite. Samples in BK-KG-10 show more chabazite than BK-KG-7. The brown silty clay is only present at trenches at which there was no siliceous silt. Its blocky structure shows signs of potential pedogenic modification (Fig 12).

Stable Isotope Analyses

The stable isotope values were determined on samples from each carbonate in each trench. These were compared to previously analyzed samples (Karis, 2012; Ashley et al., 2014b) (Fig. 13). The $\delta^{13}C$ and $\delta^{18}O$ are tightly clustered or grouped only ranging between -3.95 and -1.1 for $\delta^{18}O$ and ranging -3.89 to -2.17 for $\delta^{13}C$. The averages were

-2.46 for $\delta^{18}O$ and -1.33 for $\delta^{13}C$ (Fig. 13). The most negative results were located at Trench BK-KG-10 and the most positive results at Trench BK-KG-8. These data closely match the data previously reported by (Ashley et al., 2014b) (Fig. 13).

Clay Mineral Analyses

Clay minerals are composed of a succession of layers: a layer of silica tetrahedron with an octahedral layer, with potentially another tetrahedral layer (Fig. 14). Clay mineralogy is changed through substitution of different ions in the octahedral layer.

Clay mineralogy analysis was performed on three facies: siliceous earthy silt, waxy sandy silt, and brown silty clay. Clay XRD analysis showed each facies had one dominant clay phase (Fig. 15). The dominant clay in the siliceous earthy silt (n=9) was smectite, with 77% of samples containing smectite. The waxy sandy silts (n=7), 85% of samples were interstratified illite/smectite. For the brown silty clay, all samples (n=4) were illite-rich.

For 060 spacing and octahedral Mg values, siliceous earthy silt and brown silty clay facies showed similar results while waxy sandy silt results differed (Fig. 15). Siliceous earthy silt and brown silty clay 060 values averaged 1.51128 Å and 1.51125 Å respectively, whereas waxy sandy silt averaged 1.51503 Å. For Octahedral Mg values, siliceous earthy silt ranged from 0.7 to 1.6, mean 1.1, and brown silty clay ranges 0.9 to 1.2 with mean = 1.075. Waxy sandy silt ranged 1.1 to 2 with a mean 1.37.

XRD bulk mineralogical analysis showed siliceous earthy silt is mostly plagioclase, with augite present in 67% of samples and minor analcime, calcite, pyroxene, and zeolite present. Waxy sandy silts have a more varied geochemistry, where

in addition to plagioclase phillipsite and augite are common. Trace zeolites, chabazite, analcime, and calcite are also present. Plagioclase is present in 100% of brown silty clay samples. Quartz, augite, and analcime are also well represented. Chabazite is present in all samples, sometimes in trace quantities.

Biological Analyses

Phytolith Analysis

Of the 14 samples analyzed, 11 provided usable data (Appendix IV). However, preservation in these samples was exceptional relative to other Olduvai Gorge assemblages. Phytoliths from eight major groups were described: Grass Silica Short Cells (GSSC), grasses and sedges from families Poaceae and Cyperaceae, plants with aerial root systems, herbaceous plants from order Zingiberales, forest indicators, and palms (Fig. 16).

Grass silica short cells often formed the plurality of phytoliths in a sample, ranging from 13.9% to 33.9% and averaging 28.7% of all phytoliths. Grasses from the Pooideae subfamily (exclusively using the C3 photosynthetic pathway) were present in small quantities in three samples (BK-KG-102, BK-KG-104, BK-KG-912), ranging from 1.1% to 8% of the total phytolith assemblage.

Blocky or plate-like bodies, which are found in plants with aerating roots or stems ranged from 0% to 11.5%, averaging 3.4% of countable sample. Phytoliths such as globular granulate oblong, cork aerenchyma (honey comb bodies), and blocky or sclereid bodies are considered forest indicators. Forest indicators are present in every sample and represent an average 17.0% of total sample. Globular echinate phytoliths, which are

produced by palms (Arecaceae) are relatively scarce and were only present in 6 samples. They were abundant however in samples BK-KG-408 and BK-KG-903, where they represent 26.2% and 23.2% of total phytolith assemblage respectively.

Phytoliths of the Zingiberales, were identified for the first time at Olduvai. This botanical order comprises 8 families including Zingiberaceae (ginger, turmeric), Musaceae (bananas), Marantaceae (arrowroot), Costaceae, and others. In the samples analyzed here many types including druses, rugose hat-shapes, and knobby bodies were found, but their abundance was highly variable from sample to sample, ranging from 2.1% to 59.3% of total count, but averaging 16.1%.

Diatom Analysis

Diatoms were present in all siliceous earthy silt samples, but not in great quantities. Quantifiable assemblages of diatoms were only present in 3 out of 14 samples – BK-KG-106, BK-KG-408, and BK-KG-903 (Appendix VI). These samples come from Trenches BK-KG-1, BK-KG-4, and BK-KG-9, meaning that good conditions for diatom preservation were likely present in the northeast portion of the study area (Figs. 6, 17).

In most cases, diatoms were too fragmented to be properly identified. The maximum number of species found in a sample was 32 in sample BK-KG-408. The most common species is *Nitschia amphibia*, which represents 52%, 31.5%, and 24% of the assemblages from samples BK-KG-106, BK-KG-408, and BK-KG-903 respectively (Fig. 17). The second most well represented species is *Rhoplodia gibberula*, which comprises 4%, 8.5%, and 12% respectively. Other species present in appreciable quantities include

Synedra ulna, *Anomoeoneis sphaerphora*, *Epithermia argus*, and *Gomphonema intricatum*.

Rhizoliths

Rhizoliths were composed of 7 minerals: Opal-A, opal-CT, calcite, quartz, Mg-calcite, dolomite, and clays (Table I). The most common of these was opal-A. While either calcite, Mg-calcite, or dolomite was present on 4/7 samples, qualitative tests of these rhizoliths with HCl suggest carbonates are present in trace quantities.

DISCUSSION

Stable Isotopes

The $\delta^{13}C$ levels of incoming surface and groundwater are assumed to be -8‰, in accordance with values for modern East African rivers as detailed by (Cerling et al., 1988). Average $\delta^{18}O$ for meteoric water falling in the Ngorongoro Highlands is -4‰ (Bowen, 2010). Carbonate precipitating from this water would average -6‰ when when adjusting for the ambient ground temperature of 25° C (Coplen et al., 1983). Thus the measured ranges (-4‰ to -1‰ $\delta^{18}O$, -4‰ to 0‰ $\delta^{13}C$) show an enrichment of both ^{18}O and ^{13}C. The $\delta^{18}O$ and $\delta^{13}C$ of the carbonate deposits are clustered, although an overall covariance is apparent (Fig. 13). Both the enrichment and covariance is interpreted as the result of evaporation in a closed freshwater system (Li and Ku, 1997). The physicochemical process of evaporation causes preferential loss of ^{16}O, raising ^{18}O levels in the water body. Evaporation also raises pCO_2 of the lake, and in order to equilibrate the

lake loses CO_2 to the atmosphere. During this process ^{12}C is preferentially lost, resulting in enrichment of ^{13}C.

While photosynthetic production is a means of influencing the ^{13}C levels in a lake, in endorheic basins the influx of DIC is greater than Ca ion, and the contributory effects of photosynthetic production are too small to be seen (Benson et al., 1996). In lakes, the $\delta^{13}C$ signature is influenced by either photosynthesis or equilibration with the atmosphere. If photosynthesis were the main driver of $\delta^{13}C$, O and C signatures should be decoupled. In such systems, biologic activity acts independently of evaporation, so $\delta^{13}C$ is driven more negative while O is driven positive. This is because light carbon (^{12}C) is preferentially fixed in photosynthesis, causing the $\delta\ ^{13}C$ of DIC, and ultimately the carbonate, to increase.

If equilibration with the atmosphere is the main factor in C fractionation, C and O should be coupled. Small reservoirs equilibrate with the atmosphere, which in the Pleistocene would have put carbon isotope values around -6‰. Carbonate forming in a reservoir in full equilibrium with the atmosphere will precipitate around +2‰ (Mook et al., 1974). As evaporation drives O more positive, equilibration will drive C more positive. Modern samples of river water from the Turkana basin have been used as proxies for ancient DIC values in East Africa (Cerling et al., 1988; Liutkus et al., 2005). Cerling et al. (1988) report $\delta^{13}C$ values with a mean and mode of -10‰ with a range from -4 to -16 (VPDB). The measured range of $\delta^{13}C$ shows some carbon enrichment as a result of equilibration. The system never fully equilibrated, suggesting water was moving through the system. Excess ground water likely flowed into the nearby lake, and the carbonate was kept permanently fresh by continuous groundwater discharge.

The surrounding field relations suggest that water was entering this environment in the form of a broad zone of seepage (Ashley et al., 2014b). This is corroborated by the stable isotope data, which show little horizontal variation, suggesting no point source of water. Multiple samples were taken vertically at Trenches BK-KG-8 and BK-KG-10 (Fig. 7). These samples, combined with samples with vertical resolution collected by Ashley et al. (2014b), show no trends through time. This environment would have been fairly stable, and evaporation was a key driver of stable isotope geochemistry.

Clay Mineralogy

Deocampo (2004) used inferred octahedral Mg as a proxy for salinity, where increasing octahedral Mg values reflect substitution of Mg in increasingly saline conditions. Among the facies, siliceous earthy silt samples tended to have the lowest Mg values, ranging from 0.7 (the lowest measured value) to 1.6 with a mean of 1.1. The brown silty clay had the lowest mean at 1.075, ranging from 0.9 to 1.2. The waxy sandy silt had the highest mean at 1.37, ranging from 1.1 to 2 (Fig. 15). This suggests more saline environment of deposition for the waxy sandy silt, relative to the siliceous earthy silt and brown silty clay. The siliceous earthy silt and brown silty clay were deposited in water with similar chemistry. Octahedral Mg values of the siliceous earthy silt and brown silty clay suggest removal of Mg by fresh water. There is a positive correlation between 060 spacings and octahedral Mg values in clay samples from East Africa (Deocampo, 2004, 2015). Samples with high values indicate increasingly saline environments (Deocampo, 2004). The higher Mg and 060 values in the waxy sandy silt relative to the siliceous earthy silt and brown silty clay suggest deposition in a saline environment. One

waxy sandy silt sample, BK-KG-109, had particularly high 060 and octahedral Mg values. This sample must have formed in an alkaline, saline lake, where other samples are more equivocal. It is likely that the conditions that formed BK-KG-109 were laterally extensive in the lake. The lower 060 and octahedral Mg values of other waxy sandy silt samples are a result of minor post-depositional alteration and Mg loss.

Improvements in analytical techniques have helped elucidate the differences between clay mineral assemblages at different facies in Olduvai. Luitkus (2003) reported the siliceous earthy clay and waxy sandy silt to have nearly identical mineralogies, interpreting siliceous earthy clay products to be alterations of waxy sandy silt deposits by freshwater. In this study, the siliceous earthy silt is smectite rich, with some traces of illite, whereas the waxy sandy silt is mostly interstratified illite/smectite. Interstratified illite/smectite typically forms in saline environments, where K uptake results in illitization of smectites (Deocampo, 2015). Illite in the brown silty clay is interpreted as detrital on the basis of 060 and octahedral Mg values. In Olduvai Gorge, most illite is authigenic (Deocampo et al., 2002; Liutkus and Ashley, 2003). However, the main source of weathered detritus in this environment is the volcano Lemagurut (Fig. 4). Other studies at Olduvai Gorge describe weathered material originating from Olmoti, another NVC volcano (Fig. 4). It is possible that the source material from Lemagurut provides detrital illite, or that illite formed during weathering on the volcano before being transported and deposited in the basin.

Biological Analysis

Rhizoliths

Rhizoliths at BK are similar to those of Olorgesailie, Kenya, which were interpreted as forming in a permanently inundated wetland in a low-grade fluvial plain (Owen et al., 2009). While trace carbonate has been found in rhizolith samples, rhizoliths from the siliceous earthy silt are dominantly silica, most commonly opal-A. One source of silica for the abundant rhizoliths is from the breakdown of silicate minerals by the alkaline lake, which would have regularly inundated the wetland; other sources include volcanic glasses and other minerals, diatoms, and phytoliths (Owen et al. 2008). Opal-A is precipitated directly in plant tissues after having been taken up in plants as monosilicic acid. Plants may have been able to locally increase concentration of dissolved silica through evapotranspiration. This uptake of silica can continue even after a plant dies due to capillary forces. The natural biogenic mineralization of Opal-A combined with its concentration after death could be why the rhizoliths are dominantly opaline (Owen et al., 2008) (Fig. 18).

Diatoms

While diatoms were present in all samples analyzed, in most samples the frustules were broken and/or too scarce to provide a proper count. A Locally-Weighted Weighted Average (LWWA) transfer function run through the European Diatom Database calculated pH values ranging from 8.07-8.52 and a conductivity of 677-1753 mS for the three samples with countable diatom assemblages. These values were calculated based on counts of species in the BK diatom assemblage. Diatoms were most abundant in the NE

of the study area, having been found in trenches BK-KG-4 and BK-KG-9. The most abundant species, *Nitschia amphibia*, is a freshwater species, which indicates the siliceous earthy silt was deposited in fresh conditions (Fig. 17, Appendix 6). The presence of more saline and alkaline adapted taxa in the assemblage is likely the result of periodic (perhaps annual) flooding by the lake. This effect can be seen at Trench BK-KG-9, which had a much higher conductivity of 1753 mS, compared to 677 and 891 at trenches BK-KG-1 and BK-KG-4 respectively.

Phytoliths

The BK phytolith record shows a diverse assemblage of freshwater adapted plants and grasses. Despite the fact that grass silica short cells often comprised the plurality of phytoliths counted, the total grass input is low (always below 40% and often below 30%), and grasses are outnumbered by non-grassy plants. Thus the environment of deposition was not a grassland. Percentage of fan-shaped bulliform cells can be used as a proxy for evapotranspiration rates (Issaharou-Matchi et al., 2016). A greater percentage of fan-shaped cells indicates a greater evapotranspiration rate. The percentage of fan shaped bulliform cells is low (3.2%), which indicates the presence of a closed canopy as in a forest. This is reflected by the rarity of grasses and sedges (which produce bulliform cells) in the phytolith record (Novello et al., 2012). The presence of forest indicators (average abundance 17.0%) suggests a somewhat open environment with some tree cover. There was significant presence of plants from the Zingiberales order, in one sample (BK-KG-503) forming 59.3% of phytoliths, but averaging 13.7%. Eight botanical families belong to the Zigiberales order among which are Musaceae (banana),

Zingiberaceae (ginger, curcuma), Marantaceae (arrowroot), and others. Fruits and/or the rhizomes from these plants could have been a useful resource for hominins. Overall this microbiome can be described as a lush wetland with areas of inundated forest.

"Mangrove-like" plants with roots adapted to take CO_2 from surrounding water are not present in large quantities, but are nonetheless significant. These need permanent water to grow, suggesting that the siliceous earthy silt was perennially wet. These phytoliths are found in all but one sample, suggesting no bias for time or location in regards to permanent fresh water within the siliceous earthy silt.

Phytoliths from the BK wetland show better preservation than many older assemblages from Olduvai (D. Barboni, pers. com. December 2016). Older wetlands were continuously altered by paleo Lake Olduvai, which was at its largest in Bed I and continued to thrive in Bed II. Lake waters would percolate through and alter sediment, even long after deposition. However, the lake is not present in Bed III, meaning that there was significantly less time for the brine to alter Upper Bed II sediment. The level of preservation in the assemblage suggests phytoliths from most plants present in the wetland are represented in the phytolith record.

The phytolith assemblage points largely towards plants adapted to standing water or which live near water. Silicified bulliform cells from grass or sedge epidermis are common in plants undergoing high evapotranspiration, as would be experienced in a swamp. Silicified epidermal plates from family Cyperaceae, a family often associated with wetlands, are present. Globular echinate phytoliths from family Arecaceae (palms) grow near water, and, while rare in the assemblage, represent a taxon no longer found in the Olduvai region. More curious is the presence of trapeziform sinuate phytoliths from

high elevation Pooideae grasses, which are typically found above 2500 m elevation today (Tieszen et al., 1979). The elevation of Olduvai Gorge is ~1600 m, so these phytoliths may have been transported from the NVC. Despite this, the phytolith evidence clearly points towards a standing water environment in the siliceous earthy clay.

Facies Interpretations

Sandy Silt

The sandy silt occurs over the entire 1.5 km length of outcrop shown in Figure 6. The continuity of the sandy silt and its proximity to lacustrine deposits suggests it is either; 1) coalesced terminal splays of fluvial channels, 2) a sheet delta or 3) a littoral deposit (Renaut and Gierlowski-Kordesch, 2010) (Table 2). All of these deposits are relatively coarse grained, have little vegetation and are common along margins of siliciclastic playa lakes. The sandy silt is massive and otherwise structureless, suggesting winnowing by waves in the shallow playa lake. This environment may have been present on the north, east, and south faces of the lake while siliceous earthy silt was accumulating at the distal end of a fluvial plain (Fig. 19). The origin of this facies may be similar to sandy terminal splay delta facies at Lake Eyre in Australia (Fisher et al., 2008; Renaut and Gierlowski-Kordesch, 2010).

There were likely local changes in sediment color and grain size in lake margin deposits on different sides of the lake. While it is possible the sandy silt facies surrounded the entire lake, Hay (1970) reports the presence of gray fine-grained lake margin sediments in the Side Gorge of Bed II, which likely correspond with gray clay-rich sediments from Trench BK-KG-8 (Figs. 7, 12). Despite being clay-rich with only a minor

contribution of fine sand, this facies from trench BK-KG-8 is included in the sandy silt facies as they represent similar environments, i.e. lake margin deposits (Table 2).

Minor Tuffaceous Deposit

Above the gray clay of BK-KG-8 is a very well lithified fine grained tuff. The mineralogy and grain size of this tuff is quite distinct from the tuff found at BK-KG-10. The unit was not a good candidate for radiometric dating.

Brown silty clay

The brown silty clay occurred at only two trenches (Trenches BK-KG-7 and BK-KG-10) (Figs. 7, 11). It is stratigraphically equivalent to the siliceous earthy silt and the two facies never occur in the same trench. The contact of the facies from clay to earthy silt is not exposed, so it is not known if it is sharp or gradual. Mineralogically the brown silty clay was largely illite, as compared to the waxy sandy silt which was dominantly interstratified illite/smectite. The brown silty clay deposits are interpreted as representing quiescent pools in a delta distributary environment on the periphery of a lake (Table 2). These distributary channels were infilled with clay and fine sand. While direct evidence for only two channels was found, it is likely that more were present. The siliceous earthy silt deposited in the wetland can be seen as interfluve between distributary channels (Fig. 19). There is no evidence for significant channel migration, as these brown silty clay deposits are 60+ cm thick. As both brown silty clay deposits are overlain by tufa, the distributaries are stratigraphically equivalent to the siliceous earthy silt.

Siliceous Earthy Silt

Siliceous earthy clays were first interpreted by Hay (1976) as freshwater deposits. Although the matrix of the sediments in the study area are silts, this freshwater interpretation is supported by the diatom and phytolith assemblages, which were dominated by the freshwater diatom species *Nitschia amphibia* and freshwater plants. Whereas Hay (1976) used the term "marsh" to describe the plant-rich deposits, the term wetland is used as it is a more encompassing term including a wide range of plant types from herbaceous species to trees. This wetland would have been fed by groundwater originating as precipitation on the topographic high to the south of the basin, principally at Mt. Lemagurut (Figs. 3, 20) (Ashley et al., 2014b). The siliceous earthy silt represents parts of the wetland with abundant plant life (Table 2). The lack of discontinuities in the deposits suggests a relatively stable and continuously aggrading wet environment. The thickness of beds suggests this wetland likely existed for several hundred or few thousands of years. The siliceous nature of the deposit is due to the abundance of plant matter (i.e. siliceous rhizoliths). CO_2 released from the decay of organic matter lowers pH and inhibits calcite precipitation (Deocampo and Ashley 1999) (Fig. 16). When plant life is abundant, siliceous sediment is deposited. As the water table rises many of the plants would drown, resulting in a rise in pH and the precipitation of calcium carbonate.

Studies of other wetlands at Olduvai have interpreted siliceous earthy sediments as alteration products of waxy sandy silt beds on sedimentological and geochemical grounds (Liutkus and Ashley, 2003). This cannot be the case for this environment, as the siliceous earthy silt is of larger grain size than waxy sandy silt. Siliceous sediment for the

siliceous earthy silt was likely transported from the alluvial/fluvial system originating at Mt. Lemagurut (Figs. 3, 20).

The siliceous earthy silt is impressive (exceeding 2 m) at Trenches BK-KG-4 and BK-KG-9 (Fig. 7). This area may have been a topographic low and the local greater accommodation space would enhance sedimentation in an environment that is limited by level of water table. At Trench BK-KG-9 there was a sharp change in color in the siliceous earthy clay near a clay-filled feature that may have been an animal burrow or a termitarium, a termite nest (Fig. 9). Clay mineral analyses revealed the lower portion was poor in clay with some smectite, while the sample above had both illite and smectite present. Bulk mineralogy of the samples indicated pyroxene and plagioclase in the lower sample, with plagioclase, augite, analcime, and quartz present in the upper sample.

Carbonate

The carbonate was the only facies found at every trench (Fig. 7). It occurs at trenches with the siliceous earthy clay and with the brown silty clay (Figs. 10, 12). It is always the uppermost facies, although at some trenches it appears multiple times. The most reasonable interpretation of this facies is as pools of water in a widespread, permanently inundated wetland (Table 2). Pedley (1990) coined the term paludal wetland in which he described poorly drained environments that can be groundwater fed where "spring chalk" – micritic carbonate – coats local vegetation. Gastropods are common in these deposits and can be used for paleoenvironmental interpretation. Stable isotope results ($\delta^{18}O$ range -1.1 to -3.95‰) indicate that the carbonate was precipitated in freshwater conditions, much like the siliceous earthy silt. However, the paucity of

wetland plant remains indicates that that water was deeper than the setting in which siliceous earthy clay accumulated. At its largest, the carbonate-precipitating water body would have formed one cohesive unit at least 1.5 km x ~200 m (Fig. 6). These dimensions represent the extent of the carbonate found in outcrop and thus the minimum size of the carbonate precipitating environment. The presence of ostracods suggests well oxygenated water either gently flowing or stirred by wind (Owen et al., 2004; Ashley et al., 2014b).

The geochemical mechanism that allowed carbonate to precipitate as opposed to deposition of siliceous earthy clay was put forward by Deocampo and Ashley (1999) and is a result of the density of plant life. When plants are abundant they die and are respired by microbes. This anaerobic respiration drives up pCO_2 of local water, which converts to carbonic acid and lowers pH. Additionally, release of organic acids from the decay process lowers pH. If pH is too low, $CaCO_3$ cannot form. Calcium carbonate can only form when pH is high (i.e. plant decay is not contributing acids) and Ca^{2+} concentration is appropriate. In this way, when plant life is abundant, siliceous earthy silt is deposited. If less plant life is present, the system stops inhibiting calcite growth and the tufa deposit aggrades. Calcium ions in groundwater originate from subsurface weathering of local basalts and trachytes (Ashley et al., 2010). Thus both Ca^{+} and CO_3^{2-} are supersaturated, but the acidic effects of cellular respiration inhibit calcite growth.

Evidence for less plant life in the tufa versus the siliceous earthy clay is corroborated by sedimentology. The tufa is massive. The only structures are rhizoconcretions similar in appearance to the siliceous earthy silt before grading into a massive deposit. The best example is Trench BK-KG-2. Its micritic fabric and massive

appearance is consistent with paludal carbonates (Alonso-Zarza and Wright, 2010) and bears resemblance to tufas described in Kenya from a similar paleoenvironment (Johnson et al., 2009). The fact that this tufa is almost entirely lacking in desiccation cracks and pedogenic features suggests that it was permanently inundated.

There is no lateral or vertical variation in $\delta^{18}O$ values in the carbonates (Karis, 2012). The lack of a gradient from freshest to most evaporative localities suggests the water was discharging from a broad zone of seepage rather than from a point source (e.g. a fault), which has been the case for most other tufas at Olduvai (Ashley et al., 2014b). The most negative and thus the "freshest" carbonate stable isotope values were found at trench BK-KG-10. Here the carbonate directly overlies a brown silty clay layer, which is here interpreted as a distributary of a delta, delivering freshwater to the lake. There may have been some continued influence of fresh water in this location, resulting in negative ^{18}O values.

Waxy Sandy Silt

The term "waxy sandy silt" has long been used to describe lake clays in the Olduvai Basin (Hay, 1970; Hay, 1976; Hay and Kyser, 2001). Such clays are typically green due to the presence of smectite. Hay's research revealed that Mg-rich smectitic clays and a mineral celadonite are the principle clay minerals and that these clays suggest saline and alkaline conditions (Hay and Kyser, 2001; Hover and Ashley, 2003). Deocampo et al. (2002) used clay mineral compositions within a local area of the lake-margin and wetlands to separate saline from freshwater deposits. Waxy sandy silts are commonly found in trenches as <10 cm layers, suggesting local inundations of the lake

for several hundred years according to the sedimentation rate of non-tuff sediments in the basin (1 cm/kyr) calculated by Hay and Kyser (2001) and Ashley (2007). As a result of the low-gradient nature of the paleo Lake Olduvai, small changes in sedimentation and lake size could cause local variations in sedimentation, with waxy sandy silts being deposited for hundreds of years and switching back to siliceous silt or carbonate. Being a playa on a low-gradient plain, the lake likely covered the study area on an annual basis, but only when the lake was permanently present could waxy sandy silts accumulate.

Waxy sandy silt is the uppermost facies at most sites, where it unconformably overlies the carbonate. This suggests that the base level and water table continued to rise following the carbonate wetland phase, causing the lake to flood the wetland environment and deposit waxy sandy silt (Table 2). Thus the siliceous earthy silt – carbonate – waxy sandy silt sequence represents a continuously rising water table. The most reasonable interpretation of this persistent rising lake level and rising ground water level is a wetter climate. Wet and dry periods driven by precession cycles have been documented in the well-dated sequences in Bed I and Lowermost Bed II (Magill et al., 2013a). Precession driven climate cycles very likely occurred during Bed II time. However, correlating this sequence with the rising limb of a precession cycle requires numerical dates on the package. Single crystal argon-argon dating is in progress using the tuff exposed in Trench BK-KG-10.

Facies Model

A synthesis of the lateral and vertical facies distribution over the 1.5 km wide and >200 m wide area strongly suggests a depositional environment at the interface of a

saline and alkaline playa lake to the north and a low gradient fluvial plain to the south. The fluvial system originated on the slopes of Mt. Lemagurut and transported volcaniclastic sediment. The distal end of the fluvial system was a site of clastic deposition which might be termed a "splay delta." Splay deltas commonly occur at playa lake margins and are silty sand deposits formed when unconfined sediment-rich sheetfloods reach the lake. They deposit poorly stratified to massive sandy silt deposits and are found in underfilled lake basins (Renaut and Gierlowski-Kordesch, 2010). This sandy silt may be a littoral deposit sorted by wind and wave energy. The sandy silt became the substrate for a wetland that emerged as base level rose (Fig. 19, 21). With time the wetland was covered by an expanding paleo Lake Olduvai due to a continuously rising water table. The littoral zone of the shrunken lake during a Milankovitch minimum was quite extensive. This lake sat to the north of a broad, flat fluvial plain, wherein ephemeral streams originating on the slopes of Lemagurut formed fluvial plain deposits rich in silts and clays (Fig. 19). The water table rose and supported the sustained growth of a wetland, which supported a wide variety of plants. At this point the entirety of the wetland was depositing siliceous earthy silt. The wetland fringed the lake and existed in between distributaries of the delta. As the water table rose, pools formed, where standing water was permanent and plant life was less abundant. These pools were loci for carbonate precipitation. The system deposited mostly siliceous earthy silt with some carbonate pools (Fig. 21). Depending on local depth and sedimentation these pools may have switched back to siliceous earthy silt. Carbonate precipitating pools are localized at first, on the order of m^2 to tens of m^2, before eventually the entire system is of sufficient depth to precipitate carbonate. At this time the delta distributaries are inundated by this

carbonate precipitating system. The top of the sequence recorded an expansion of the saline-alkaline playa lake water that flooded onto the terminus of the fluvial plain and drowned the paludal wetland and stopped carbonate accumulation.

Paleoenvironmental Context

This is the first wetland described at Olduvai to occur as part of a fluvial/playa lake system. Previous wetlands described at Olduvai Gorge were groundwater-fed either at the distal end of the alluvial plain (Fig. 20) (Ashley et al., 2016), or on the margin flats (Liutkus and Ashley, 2003), or adjacent to faults (Ashley et al., 2014b). Most have occurred during waning (wet to dry) precessional limbs (Deocampo, 2002a; Liutkus and Ashley, 2003) (Fig. 22). These wetlands begin when lake levels were low and precipitation from Olmoti during the previous maximum has had a chance to move through the groundwater system and seep out near the lake or emerge through a fault (Deocampo, 2002a; Ashley et al., 2014b). Wetlands are flooded by lakes during precession maxima when lake level rises again. This wetland, however, formed during a waxing limb (Fig. 22). The increased precipitation had an immediate effect on the groundwater system, increasing the rate of discharge and forming a wetland that grew more expansive and deep as rainfall increased.

CONCLUSIONS

Observations of sedimentary successions, mineralogy, biological remains, and stable isotope analyses from 10 trenches spread over 1.5 km suggests the environment of

deposition was a lush wetland that formed at the terminus of a low-gradient fluvial system. The five lithofacies identified (sandy silt, brown silty clay, siliceous earthy silt, tufa, waxy green clay) provide the architectural elements of the lacustrine delta facies model. The wetland formed on sandy splay delta sediments (or sandy littoral deposits) on the margin of a saline-alkaline playa lake, an area of very low accommodation space.

This wetland formed on a dry-wet limb of a precession cycle. Sourced by groundwater and seasonal surface water, silica rich waters led to the preservation of rhizoliths and diatoms. Fresh water supported grass and palm species that could not have otherwise grown in the arid grasslands of the adjacent Serengeti. Continuous discharge of groundwater originating in Mt. Lemagurut kept the wetland permanently inundated. Fluvial sediment from the same source was transported fines to the wetland and also formed distributary channels which cut through the wetland, depositing brown silty clay. Brown silty clay deposits are interpreted as being deposited in localized pools on the basis of their clay mineralogy, which suggests freshwater and detrital sediment. Carbonate was deposited initially in pools of greater depth than the siliceous earthy silt, where a lack of standing plant life changed local water chemistry and allowed for carbonate deposition. A rising water table caused pervasive carbonate deposition in the wetland, resulting in a tufa. Carbonate $\delta^{18}O$ values indicate that the carbonate was precipitated from groundwater sourced from meteoric rainfall. Ultimately, base level rose to the point where the lake flooded the wetland. Waxy sandy silts form the top of the sedimentary sequence.

In an arid environment, fresh water would have been an important resource for hominins. Both *Homo erectus* and *Paranthropus boisei* may have taken advantage of this

wetland, as evidenced by their activity at the two nearby paleoanthropological sites of BK and SC. At BK, *Homo erectus* butchered medium and large size game. The fresh water, shade, and plant resources provided by the wetland likely would have been attractive to hominins.

REFERENCES

Albert, R. M., and Bamford, M. K., 2012, Vegetation during UMBI and deposition of Tuff IF at Olduvai Gorge, Tanzania (ca. 1.8 Ma) based on phytoliths and plant remains: Journal of Human Evolution, v. 63, no. 2, p. 342-350.

Alonso-Zarza, A. M., 2003, Palaeoenvironmental significance of palustrine carbonates and calcretes in the geological record: Earth-Science Reviews, v. 60, no. 3, p. 261-298.

Alonso-Zarza, A. M., and Wright, V., 2010, Palustrine carbonates: Developments in Sedimentology, v. 61, p. 103-131.

Arenas, C., Cabrera, L., and Ramos, E., 2007, Sedimentology of tufa facies and continental microbialites from the Palaeogene of Mallorca Island (Spain): Sedimentary Geology, v. 197, no. 1, p. 1-27.

Ashley, G. M., 2007, Orbital rhythms, monsoons, and playa lake response, Olduvai Basin, equatorial East Africa (ca. 1.85–1.74 Ma): Geology, v. 35, no. 12.

Ashley, G. M., Barboni, D., Dominguez-Rodrigo, M., Bunn, H. T., Mabulla, A. Z. P., Diez-Martin, F., Barba, R., and Baquedano, E., 2010, A spring and wooded habitat at FLK Zinj and their relevance to origins of human behavior: Quaternary Research, v. 74, no. 3, p. 304-314.

Ashley, G. M., Beverly, E. J., Sikes, N. E., and Driese, S. G., 2014a, Paleosol diversity in the Olduvai Basin, Tanzania: Effects of geomorphology, parent material, depositional environment, and groundwater on soil development: Quaternary International, v. 322-323, p. 66-77.

Ashley, G. M., de Wet, C. B., Barboni, D., and Magill, C. R., 2016, Subtle signatures of seeps: Record of groundwater in a dryland, DK, Olduvai Gorge, Tanzania: The Depositional Record.

Ashley, G. M., De Wet, C. B., Dominguez-Rodrigo, M., Karis, A. M., O'Reilly, T. M., and Baluyot, R., 2014b, Freshwater Limestone In An Arid Rift Basin: A Goldilocks Effect: Journal of Sedimentary Research, v. 84, no. 11, p. 988-1004.

Ashley, G. M., and Hay, R. L., 2002, Sedimentation patterns in a Plio-Pleistocene volcaniclastic rift-platform basin, Olduvai Gorge, Tanzania: Sedimentation in Continental Rifts, SEPM Special Publication 73, p. 107-122.

Ashley, G. M., Tactikos, J. C., and Owen, R. B., 2009, Hominin use of springs and wetlands: Paleoclimate and archaeological records from Olduvai Gorge (~1.79–1.74 Ma): Palaeogeography, Palaeoclimatology, Palaeoecology, v. 272, no. 1-2, p. 1-16.

Bamford, M. K., 2005, Early Pleistocene fossil wood from Olduvai Gorge, Tanzania: Quaternary International, v. 129, no. 1, p. 15-22.

Barboni, D., 2014, Vegetation of Northern Tanzania during the Plio-Pleistocene: A synthesis of the paleobotanical evidences from Laetoli, Olduvai, and Peninj hominin sites: Quaternary International, v. 322-323, p. 264-276.

Barboni, D., Ashley, G. M., Dominguez-Rodrigo, M., Bunn, H. T., Mabulla, A. Z., and Baquedano, E., 2010, Phytoliths infer locally dense and heterogeneous

paleovegetation at FLK North and surrounding localities during upper Bed I time, Olduvai Gorge, Tanzania: Quaternary Research, v. 74, no. 3, p. 344-354.
Benson, L., White, L. D., and Rye, R., 1996, Carbonate deposition, Pyramid Lake Subbasin, Nevada: 4. Comparison of the stable isotope values of carbonate deposits (tufas) and the Lahontan lake-level record: Palaeogeography, Palaeoclimatology, Palaeoecology, v. 122, no. 1, p. 45-76.
Beverly, E. J., Ashley, G. M., and Driese, S. G., 2014, Reconstruction of a Pleistocene paleocatena using micromorphology and geochemistry of lake margin paleo-Vertisols, Olduvai Gorge, Tanzania: Quaternary International, v. 322-323, p. 78-94.
Blumenschine, R. J., and Peters, C. R., 1998, Archaeological predictions for hominid land use in the paleo-Olduvai Basin, Tanzania, during lowermost Bed II times: Journal of Human Evolution, v. 34, no. 6, p. 565-608.
Bonnefille, R., 1984, Palynological research at Olduvai Gorge: National Geographic Society Research Reports, v. 17, p. 227-243.
Bowen, G., 2010, The online isotopes in precipitation calculator, Version.
Bunn, H., Mabulla, A., Domínguez-Rodrigo, M., Ashley, G., Barba, R., Diez-Martin, F., Remer, K., Yravedra, J., and Baquedano, E., 2010, Was FLK North levels 1–2 a classic “living floor” of Oldowan hominins or a taphonomically complex palimpsest dominated by large carnivore feeding behavior?: Quaternary Research, v. 74, no. 3, p. 355-362.
Cane, M. A., and Molnar, P., 2001, Closing of the Indonesian seaway as a precursor to east African aridification around 3–4 million years ago: Nature, v. 411, no. 6834, p. 157-162.
Cerling, T. E., Bowman, J. R., and O'Neil, J. R., 1988, An isotopic study of a fluvial-lacustrine sequence: The Plio-Pleistocene koobi fora sequence, East Africa: Palaeogeography, Palaeoclimatology, Palaeoecology, v. 63, no. 4, p. 335-356.
Cerling, T. E., Harris, J. M., MacFadden, B. J., Leakey, M. G., Quade, J., Eisenmann, V., and Ehleringer, J. R., 1997, Global vegetation change through the Miocene/Pliocene boundary: Nature, v. 389, no. 6647, p. 153-158.
Cerling, T. E., Wang, Y., and Quade, J., 1993, Expansion of C4 ecosystems as an indicator of global ecological change in the late Miocene: Nature, v. 361, no. 6410, p. 344-345.
Copeland, S. R., 2007, Vegetation and plant food reconstruction of lowermost Bed II, Olduvai Gorge, using modern analogs: Journal of Human Evolution, v. 53, no. 2, p. 146-175.
Coplen, T. B., Kendall, C., and Hopple, J., 1983, Comparison of stable isotope reference samples.
Cuthbert, M. O., and Ashley, G. M., 2014, A spring forward for hominin evolution in East Africa: PLoS One, v. 9, no. 9, p. e107358.
Dart, R. A., 1925, Australopithecus africanus: The man-ape of South Africa: Nature, v. 115, no. 2884, p. 195-199.
Dawson, J. B., The Gregory rift valley and Neogene-recent volcanoes of northern Tanzania 2008, Geological Society of London, No. 33, p. 102
Deino, A., Kingston, J., Glen, J., Edgar, R., and Hill, A., 2006, Precessional forcing of lacustrine sedimentation in the late Cenozoic Chemeron Basin, Central Kenya

Rift, and calibration of the Gauss/Matuyama boundary: Earth and Planetary Science Letters, v. 247, no. 1-2, p. 41-60.
Deino, A. L., 2012, (40)Ar/(39)Ar dating of Bed I, Olduvai Gorge, Tanzania, and the chronology of early Pleistocene climate change: J Hum Evol, v. 63, no. 2, p. 251-273.
deMenocal, P. B., 1995, Plio-Pleistocene African climate: Science (New York, NY), v. 270, no. 5233, p. 53-59.
Deocampo, D., Cuadros, J., Wing-Dudek, T., Olives, J., and Amouric, M., 2009, Saline lake diagenesis as revealed by coupled mineralogy and geochemistry of multiple ultrafine clay phases: Pliocene Olduvai Gorge, Tanzania: American Journal of Science, v. 309, no. 9, p. 834-868.
Deocampo, D. M., 2002a, Sedimentary processes and lithofacies in lake-margin groundwater-fed wetlands in East Africa.
-, 2002b, Sedimentary processes and lithofacies in lake-margin groundwater-fed wetlands in East Africa: SEPM Special Publication, No. 73, p. 295-308.
-, 2004, Authigenic clays in East Africa: regional trends and paleolimnology at the Plio–Pleistocene boundary, Olduvai Gorge, Tanzania: Journal of Paleolimnology, v. 31, no. 1, p. 1-9.
-, 2015, Authigenic clay minerals in lacustrine mudstones: Geological Society of America Special Papers, v. 515, p. SPE515-503.
Deocampo, D. M., and Ashley, G. M., 1999, Siliceous islands in a carbonate sea: modern and Pleistocene spring-fed wetlands in Ngorongoro Crater and Oldupai Gorge, Tanzania: Journal of Sedimentary Research, v. 69, no. 5.
Deocampo, D. M., Behrensmeyer, A. K., and Potts, R., 2010, Ultrafine clay minerals of the Pleistocene Olorgesailie Formation, southern Kenya Rift: diagenesis and paleoenvironments of early hominins: Clays and Clay Minerals, v. 58, no. 3, p. 294-310.
Deocampo, D. M., Blumenschine, R. J., and Ashley, G. M., 2002, Wetland Diagenesis and Traces of Early Hominids, Olduvai Gorge, Tanzania: Quaternary Research, v. 57, no. 2, p. 271-281.
Dominguez-Rodrigo, M., Mabulla, A., Bunn, H. T., Barba, R., Diez-Martin, F., Egeland, C. P., Espilez, E., Egeland, A., Yravedra, J., and Sanchez, P., 2009, Unraveling hominin behavior at another anthropogenic site from Olduvai Gorge (Tanzania): new archaeological and taphonomic research at BK, Upper Bed II: J Hum Evol, v. 57, no. 3, p. 260-283.
Dominguez-Rodrigo, M., Pickering, T. R., Baquedano, E., Mabulla, A., Mark, D. F., Musiba, C., Bunn, H. T., Uribelarrea, D., Smith, V., Diez-Martin, F., Perez-Gonzalez, A., Sanchez, P., Santonja, M., Barboni, D., Gidna, A., Ashley, G., Yravedra, J., Heaton, J. L., and Arriaza, M. C., 2013, First partial skeleton of a 1.34-million-year-old Paranthropus boisei from Bed II, Olduvai Gorge, Tanzania: PLoS One, v. 8, no. 12, p. e80347.
Etler, D. A., 1996, The fossil evidence for human evolution in Asia: Annual Review of Anthropology, p. 275-301.
Fernandez-Jalvo, Y., Denys, C., Andrews, P., Williams, T., Dauphin, Y., and Humphrey, L., 1998, Taphonomy and palaeoecology of Olduvai bed-I (Pleistocene, Tanzania): Journal of Human Evolution, v. 34, no. 2, p. 137-172.

Fisher, J. A., Krapf, C. B., Lang, S. C., Nichols, G. J., and Payenberg, T. H., 2008, Sedimentology and architecture of the Douglas Creek terminal splay, Lake Eyre, central Australia: Sedimentology, v. 55, no. 6, p. 1915-1930.

Ford, T., and Pedley, H., 1996, A review of tufa and travertine deposits of the world: Earth-Science Reviews, v. 41, no. 3, p. 117-175.

Foster, A., Ebinger, C., Mbede, E., and Rex, D., 1997, Tectonic development of the northern Tanzanian sector of the East African Rift System: Journal of the Geological Society, v. 154, no. 4, p. 689-700.

Gasse, F., 1986, East African diatoms : taxonomy, ecological distribution, Berlin, J. Cramer, Bibliotheca Diatomologica, v. Bd 11, 201 p., [288] p. of plates p.:

Hay, R. L., 1970, Silicate reactions in three lithofacies of a semi-arid basin, Olduvai Gorge, Tanzania: Mineralogical Society of America Special Paper, v. 3, p. 237-255.

Hay, R. L., 1976, Geology of the Olduvai Gorge : a study of sedimentation in a semiarid basin, Berkeley, University of California Press, xvi, 203 p., [214] leaves of plates (206 fold.) p.:

Hay, R. L., and Kyser, T. K., 2001, Chemical sedimentology and paleoenvironmental history of Lake Olduvai, a Pliocene lake in northern Tanzania: Geological Society of America Bulletin, v. 113, no. 12, p. 1505-1521.

Hover, V. C., and Ashley, G. M., 2003, Geochemical signatures of paleodepositional and diagenetic environments: a STEM/AEM study of authigenic clay minerals from an arid rift basin, Olduvai Gorge, Tanzania: Clays and Clay Minerals, v. 51, no. 3, p. 231-251.

Issaharou-Matchi, I., Barboni, D., Meunier, J.-D., Saadou, M., Dussouillez, P., Contoux, C., and Zirihi-Guede, N., 2016, Intraspecific biogenic silica variations in the grass species Pennisetum pedicellatum along an evapotranspiration gradient in South Niger: Flora-Morphology, Distribution, Functional Ecology of Plants, v. 220, p. 84-93.

Jackson, M. L., 1969, Soil chemical analysis : advanced course, [S.l., s. n.], xiii, 895 p. p.:

Johnson, C. R., Ashley, G. M., De Wet, C. B., Dvoretsky, R., Park, L., Hover, V. C., Bernhart Owen, R., and McBrearty, S., 2009, Tufa as a record of perennial fresh water in a semi-arid rift basin, Kapthurin Formation, Kenya: Sedimentology, v. 56, no. 4, p. 1115-1137.

Jung, G., Prange, M., and Schulz, M., 2015, Influence of topography on tropical African vegetation coverage: Climate Dynamics, v. 46, no. 7-8, p. 2535-2549.

Karis, A. M., Spartial and Temporal Variability of Stable Isotopes in an Upper Bed II Tufa, Olduvai Gorge, Tanzania. GSA Abstracts with Programs Vol. 44, No. 7, p. 239. 2012.

Kingston, J. D., and Hill, A., 2006, When it Rains it Pours: Legends and Realities of the East African Pluvials.

Kovarovic, K., Slepkov, R., and McNulty, K. P., 2013, Ecological continuity between lower and upper bed II, Olduvai Gorge, Tanzania: Journal of Human Evolution, v. 64, no. 6, p. 538-555.

Le Gall, B., Nonnotte, P., Rolet, J., Benoit, M., Guillou, H., Mousseau-Nonnotte, M., Albaric, J., and Deverchère, J., 2008, Rift propagation at craton margin.:

Distribution of faulting and volcanism in the North Tanzanian Divergence (East Africa) during Neogene times: Tectonophysics, v. 448, no. 1, p. 1-19.
Leakey, L. S., Tobias, P. V., and Napier, J. R., 1964, A new species of the genus Homo from Olduvai Gorge.
Leakey, L. S. B., 1959, A New Fossil Skull From Olduvai: Nature, v. 184, no. 4685, p. 491-493.
-, 1965, Olduvai Gorge, 1951-61, Cambridge [Eng.],, University Press.
Leakey, M. D., 1971, Olduvai Gorge. Vol. 3, Excavations in Beds I and II, 1960-63, Cambridge University Press.
Leakey, M. D., 1979, Olduvai Gorge : my search for early man, London, Collins, 187 p. p.:
Li, H.-C., and Ku, T.-L., 1997, δ 13 C–δ 18 C covariance as a paleohydrological indicator for closed-basin lakes: Palaeogeography, Palaeoclimatology, Palaeoecology, v. 133, no. 1, p. 69-80.
Liutkus, C. M., and Ashley, G. M., 2003, Facies model of a semiarid freshwater wetland, Olduvai Gorge, Tanzania: Journal of Sedimentary Research, v. 73, no. 5, p. 691-705.
Liutkus, C. M., Wright, J. D., Ashley, G. M., and Sikes, N. E., 2005, Paleoenvironmental interpretation of lake-margin deposits using δ13C and δ18O results from early Pleistocene carbonate rhizoliths, Olduvai Gorge, Tanzania: Geology, v. 33, no. 5, p. 377.
Madella, M., Alexandré, A., Ball, T., and Group, I. W., 2005, International code for phytolith nomenclature 1.0: Annals of Botany, v. 96, no. 2, p. 253-260.
Magill, C. R., Ashley, G. M., Dominguez-Rodrigo, M., and Freeman, K. H., 2016, Dietary options and behavior suggested by plant biomarker evidence in an early human habitat: Proc Natl Acad Sci U S A, p. 2874-2879.
Magill, C. R., Ashley, G. M., and Freeman, K. H., 2013a, Ecosystem variability and early human habitats in eastern Africa: Proc Natl Acad Sci U S A, v. 110, no. 4, p. 1167-1174.
Magill, C. R., Ashley, G. M., and Freeman, K. H., 2013b, Water, plants, and early human habitats in eastern Africa: Proceedings of the National Academy of Sciences, v. 110, no. 4, p. 1175-1180.
Maslin, M. A., Brierley, C. M., Milner, A. M., Shultz, S., Trauth, M. H., and Wilson, K. E., 2014, East African climate pulses and early human evolution: Quaternary Science Reviews, v. 101, p. 1-17.
McHenry, L. J., 2005, Phenocryst composition as a tool for correlating fresh and altered tephra, Bed I, Olduvai Gorge, Tanzania: Stratigraphy, v. 2, no. 2, p. 101-115.
McHenry, L. J., Mollel, G. F., and Swisher, C. C., 2008, Compositional and textural correlations between Olduvai Gorge Bed I tephra and volcanic sources in the Ngorongoro Volcanic Highlands, Tanzania: Quaternary International, v. 178, no. 1, p. 306-319.
McHenry, L. J., Njau, J. K., de la Torre, I., and Pante, M. C., 2016, Geochemical “fingerprints” for Olduvai Gorge Bed II tuffs and implications for the Oldowan–Acheulean transition: Quaternary Research, v. 85, no. 1, p. 147-158.

Miao, Y., Herrmann, M., Wu, F., Yan, X., and Yang, S., 2012, What controlled Mid–Late Miocene long-term aridification in Central Asia? — Global cooling or Tibetan Plateau uplift: A review: Earth-Science Reviews, v. 112, no. 3-4, p. 155-172.

Molnar, P., England, P., and Martinod, J., 1993, Mantle dynamics, uplift of the Tibetan Plateau, and the Indian monsoon: Reviews of Geophysics, v. 31, no. 4, p. 357-396.

Mook, W., Bommerson, J., and Staverman, W., 1974, Carbon isotope fractionation between dissolved bicarbonate and gaseous carbon dioxide: Earth and Planetary Science Letters, v. 22, no. 2, p. 169-176.

Moore, D. M., and Reynolds, R. C., 1989, X-ray Diffraction and the Identification and Analysis of Clay Minerals, Oxford University Press, 332 p.:

Nicholas, G., 2013, Towards an anthropology of wetland archaeology: Hunters-gatherers and wetlands in theory and practice: The Oxford Handbook of Wetland Archaeology. Oxford University Press, Oxford, p. 76.

Novello, A., Barboni, D., Berti-Equille, L., Mazur, J.-C., Poilecot, P., and Vignaud, P., 2012, Phytolith signal of aquatic plants and soils in Chad, Central Africa: Review of Palaeobotany and Palynology, v. 178, p. 43-58.

Owen, R., Renaut, R., Hover, V., Ashley, G., and Muasya, A., 2004, Swamps, springs and diatoms: wetlands of the semi-arid Bogoria-Baringo Rift, Kenya: Hydrobiologia, v. 518, no. 1-3, p. 59-78.

Owen, R. A., Owen, R. B., Renaut, R. W., Scott, J. J., Jones, B., and Ashley, G. M., 2008, Mineralogy and origin of rhizoliths on the margins of saline, alkaline Lake Bogoria, Kenya Rift Valley: Sedimentary Geology, v. 203, no. 1-2, p. 143-163.

Owen, R. B., Renaut, R. W., Scott, J. J., Potts, R., and Behrensmeyer, A. K., 2009, Wetland sedimentation and associated diatoms in the Pleistocene Olorgesailie Basin, southern Kenya Rift Valley: Sedimentary Geology, v. 222, no. 1-2, p. 124-137.

Pagani, M., Freeman, K. H., and Arthur, M. A., 1999, Late Miocene atmospheric CO2 concentrations and the expansion of C4 grasses: Science, v. 285, no. 5429, p. 876-879.

Pedley, H., 1990, Classification and environmental models of cool freshwater tufas: Sedimentary Geology, v. 68, no. 1, p. 143-154.

Pigati, J. S., Rech, J. A., Quade, J., and Bright, J., 2014, Desert wetlands in the geologic record: Earth-Science Reviews, v. 132, p. 67-81.

Plummer, T. W., and Bishop, L. C., 1994, Hominid paleoecology at Olduvai Gorge, Tanzania as indicated by antelope remains: Journal of Human Evolution, v. 27, no. 1, p. 47-75.

Poppe, L., Paskevich, V., Hathaway, J., and Blackwood, D., 2001, A laboratory manual for X-ray powder diffraction: US Geological Survey Open-File Report, v. 1, no. 041, p. 1-88.

Potts, R., 1994, Variables versus models of early Pleistocene hominid land use: Journal of Human Evolution, v. 27, no. 1, p. 7-24.

-, 2013, Hominin evolution in settings of strong environmental variability: Quaternary Science Reviews, v. 73, p. 1-13.

Quade, J., Cerling, T. E., and Bowman, J. R., 1989, Development of Asian monsoon revealed by marked ecological shift during the latest Miocene in northern Pakistan: Nature, v. 342, no. 6246, p. 163-166.

Quade, J., Mifflin, M. D., Pratt, W. L., McCoy, W., and Burckle, L., 1995, Fossil spring deposits in the southern Great Basin and their implications for changes in water-table levels near Yucca Mountain, Nevada, during Quaternary time: Geological Society of America Bulletin, v. 107, no. 2, p. 213-230.

Quade, J., Rech, J. A., Betancourt, J. L., Latorre, C., Quade, B., Rylander, K. A., and Fisher, T., 2008, Paleowetlands and regional climate change in the central Atacama Desert, northern Chile: Quaternary Research, v. 69, no. 3, p. 343-360.

Rea, D. K., Snoeckx, H., and Joseph, L. H., 1998, Late Cenozoic Eolian deposition in the North Pacific: Asian drying, Tibetan uplift, and cooling of the northern hemisphere: Paleoceanography, v. 13, no. 3, p. 215-224.

Rech, J. A., Quade, J., and Betancourt, J. L., 2002, Late Quaternary paleohydrology of the central Atacama Desert (lat 22–24 S), Chile: Geological Society of America Bulletin, v. 114, no. 3, p. 334-348.

Reck, H., 1951, A preliminary survey of the tectonics and stratigraphy of Olduvai, Cambridge University Press, London, p. 5-19.

Renaut, R. W., and Gierlowski-Kordesch, E. H., 2010, Lakes: Facies models, v. 4, Chapter 2, p. 541-575.

Richmond, B. G., and Jungers, W. L., 2008, Orrorin tugenensis Femoral Morphology and the Evolution of Hominin Bipedalism: Science, v. 319, no. 5870, p. 1662-1665.

Ruddiman, W., 2000, Earth's Climate-past and future: New York. 441p.

Ruddiman, W., Raymo, M., Lamb, H., and Andrews, J., 1988, Northern hemisphere climate regimes during the past 3 Ma: possible tectonic connections [and discussion]: Philosophical Transactions of the Royal Society B: Biological Sciences, v. 318, no. 1191, p. 411-430.

Selley, R., 1997, The basins of Northwest Africa: structural evolution: Sedimentary Basins of the World, v. 3, p. 17-26.

Sommerfeld, A., Prömmel, K., and Cubasch, U., 2014, The East African Rift System and the impact of orographic changes on regional climate and the resulting aridification: International Journal of Earth Sciences, v. 105, no. 6, p. 1779-1794.

Springer, A. E., and Stevens, L. E., 2008, Spheres of discharge of springs: Hydrogeology Journal, v. 17, no. 1, p. 83-93.

Stollhofen, H., and Stanistreet, I. G., 2012, Plio-Pleistocene synsedimentary fault compartments, foundation for the eastern Olduvai Basin paleoenvironmental mosaic, Tanzania: Journal of Human Evolution, v. 63, no. 2, p. 309-327.

Tieszen, L. L., Senyimba, M. M., Imbamba, S. K., and Troughton, J. H., 1979, The distribution of C3 and C4 grasses and carbon isotope discrimination along an altitudinal and moisture gradient in Kenya: Oecologia, v. 37, no. 3, p. 337-350.

Tooth, S., and McCarthy, T. S., 2007, Wetlands in drylands: geomorphological and sedimentological characteristics, with emphasis on examples from southern Africa: Progress in Physical Geography, v. 31, no. 1, p. 3-41.

Trauth, M. H., Maslin, M. A., Deino, A., and Strecker, M. R., 2005, Late cenozoic moisture history of East Africa: Science, v. 309, no. 5743, p. 2051-2053.

Zollikofer, C. P. E., Ponce de Leon, M. S., Lieberman, D. E., Guy, F., Pilbeam, D., Likius, A., Mackaye, H. T., Vignaud, P., and Brunet, M., 2005, Virtual cranial reconstruction of Sahelanthropus tchadensis: Nature, v. 434, no. 7034, p. 755-759.

TABLES

Table 1: Rhizolith mineralogy results

Sample	Calcite	Quartz	Opal-A	Opal-CT	Mg-Calcite	Dolomite	Clay
White_1	x	x	x	x			x
White_2			x				x
White_3			x	x			
White_4					x		trace
White_5	x					x	
White_6					x		
White_7		?	x	x	x		

Table 2: Facies Descriptions and Interpretations

Facies	Color	Description	Clay Mineralogy	Depositional Environment
Siliceous Earthy Silt	2.5Y 7/3 5 to 2.5Y 8/1	Abundant with signs of life. Opaline rhizoliths, phytoliths, diatoms, occasional vertebrate fossils	Smectite	Wetland, water pH range 6-7
Waxy Sandy Silt	2.5Y 2/3 to 5Y 5/3	Massive. Typically forms layers ~10 cm thick. Usually found above the carbonate	Illite/Smectite	Saline, alkaline lake, pH range 8-9
Dark Silty Clay	5Y 6/3 to 5Y 4/3	Only found in trenches without siliceous earthy silt. Massive.	Illite	Lacustrine delta, pH ~7
Carbonate	White to off-white	Dense, well lithified micrite with some nodules	Carbonate	Pools within wetland, pH 7-8
Silty Sand	5Y 8/2	Massive, with some vertebrate fossils. Sand fraction is rich in mafic grains.	Not analyzed	Lake margin/splay delta

FIGURES

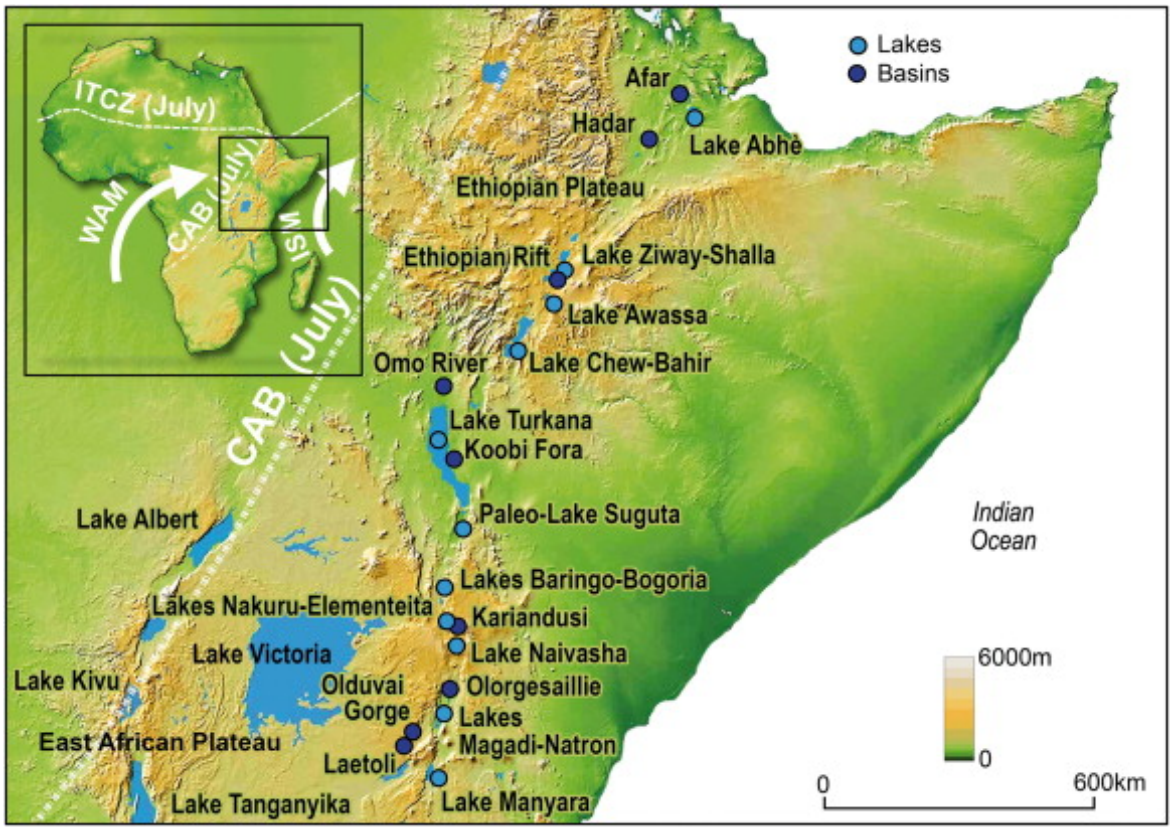

Fig. 1: Map of East Africa, highlighting rift lakes and archaeological sites in the East African Rift System from Ethiopia to Tanzania. From Maslin et al. (2014).

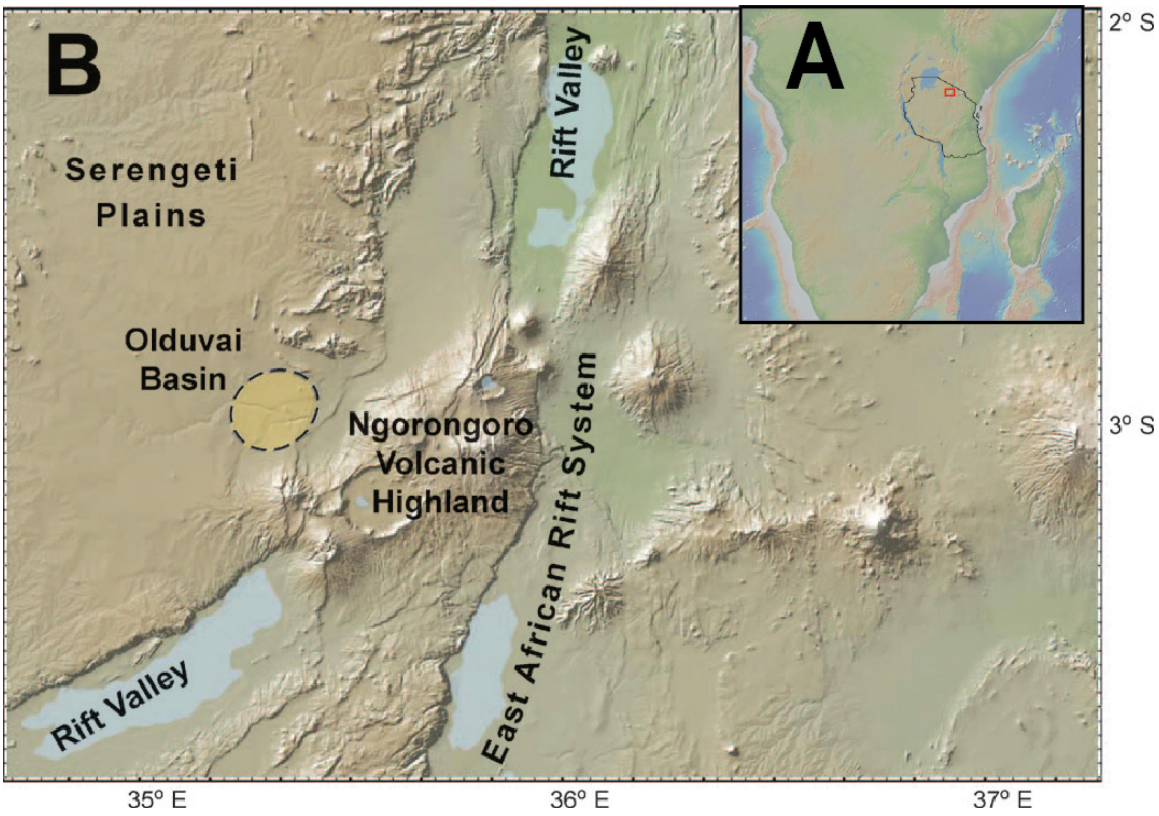

Fig. 2: A: Inset showing outline of Tanzania on African continent and red outline of larger map. B: Geomapapp image of the Olduvai region. The position of the Ngorongoro Volcanic Complex is shown relative to the EARS and the Olduvai Basin. The Serengeti sits to the NW. Modified from Ashley et al. (2014b).

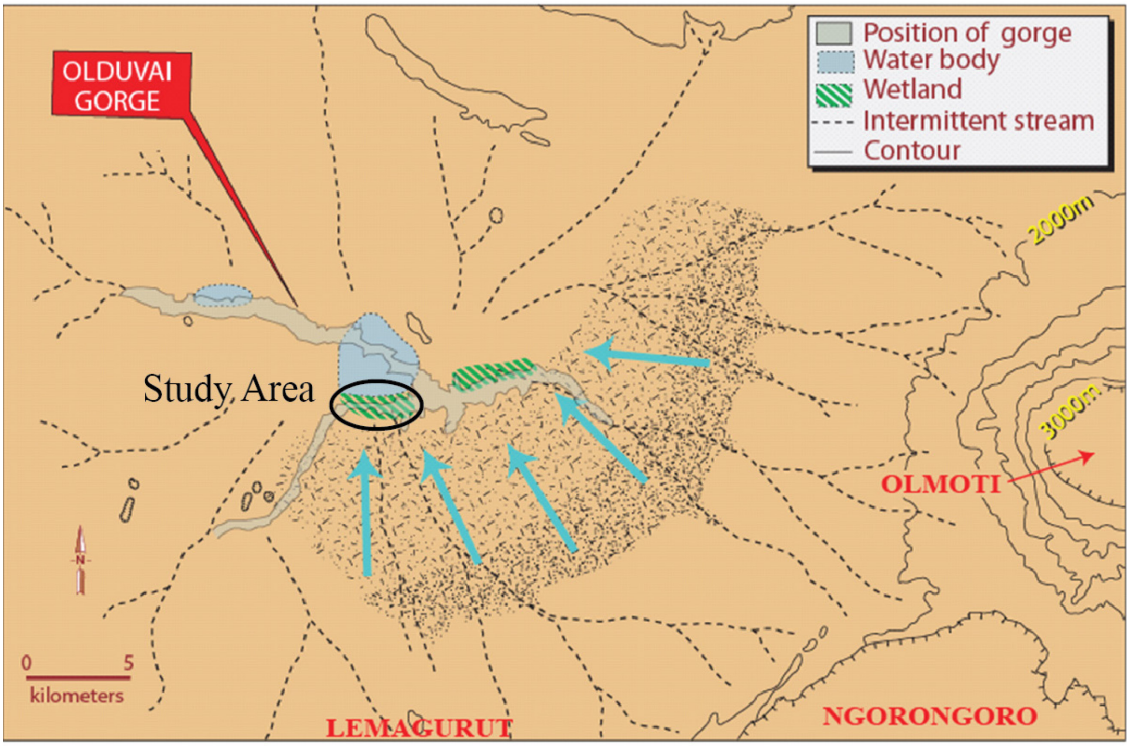

Fig. 3: Reconstruction of Olduvai Paleoenvironment after deposition of Tuff IID. Lemagurut, Ngorongoro, and Olmoti are volcanoes in the NVC. The blue arrows represent the flow of water from the Ngorongoro highlands to the Olduvai basin. Study area, in the Side Gorge, is circled in black. From Hay (1976)

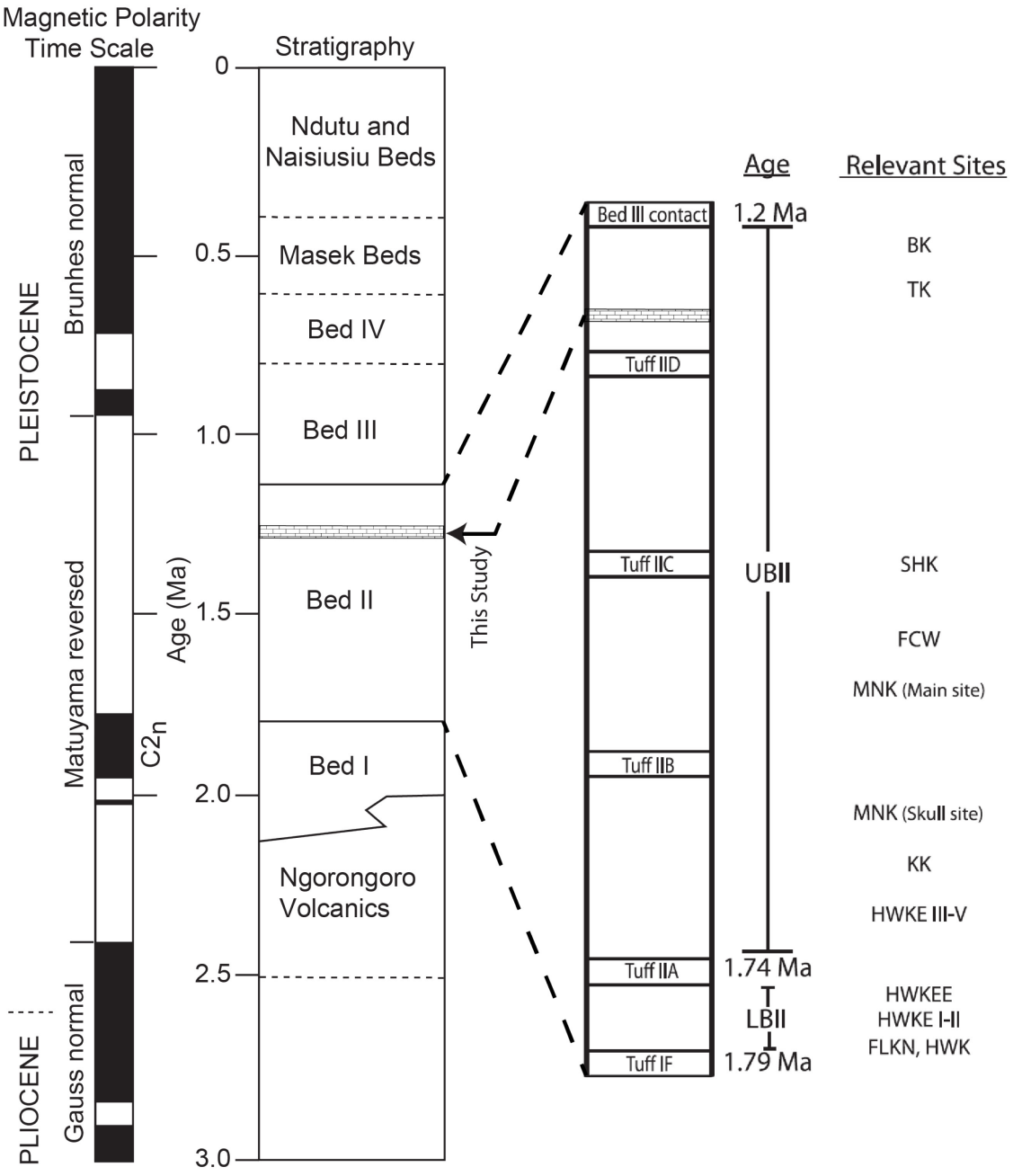

Fig. 4: Geologic column of the Olduvai stratigraphy with Magnetic Stratigraphy and absolute dates. Modified from Hay (1976) and Kovarovic et al. (2013).

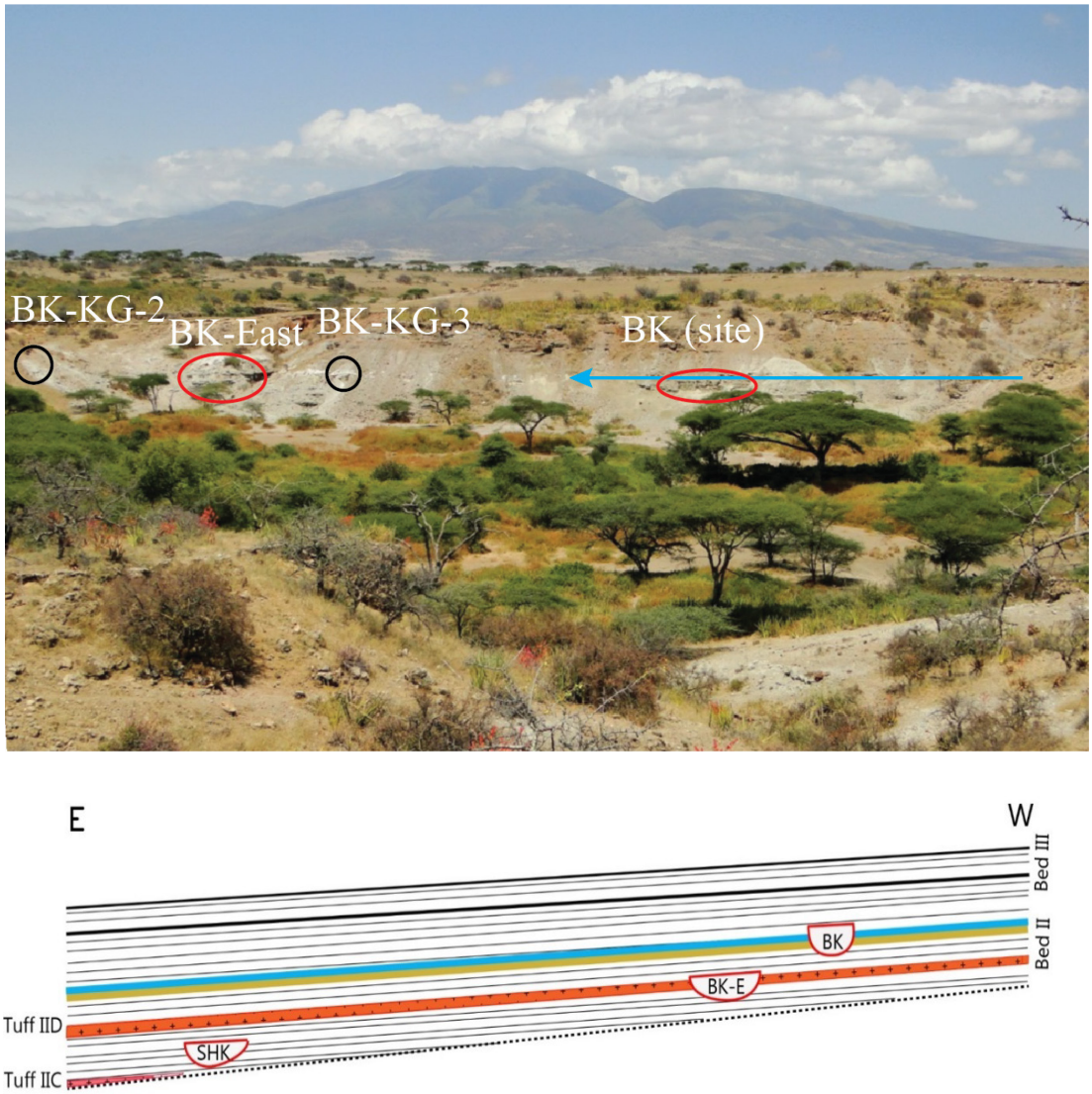

Fig. 5: Photograph taken from the north side of the gorge looking south to the BK area. The location of the BK and BK-East paleoanthropological sites are circled (red), as are the locations of Trenches BK-KG-2 and BK-KG-3 (black). The blue arrow indicates the level of the carbonate, which can be traced throughout much of the Side Gorge. The volcano Lemagurut is seen in the distance. Below: Cross-sectional depiction of bedding in the Side Gorge with exaggerated dip. The fluvial context sites BK and BK East are shown relative to the target unit (in blue and yellow).

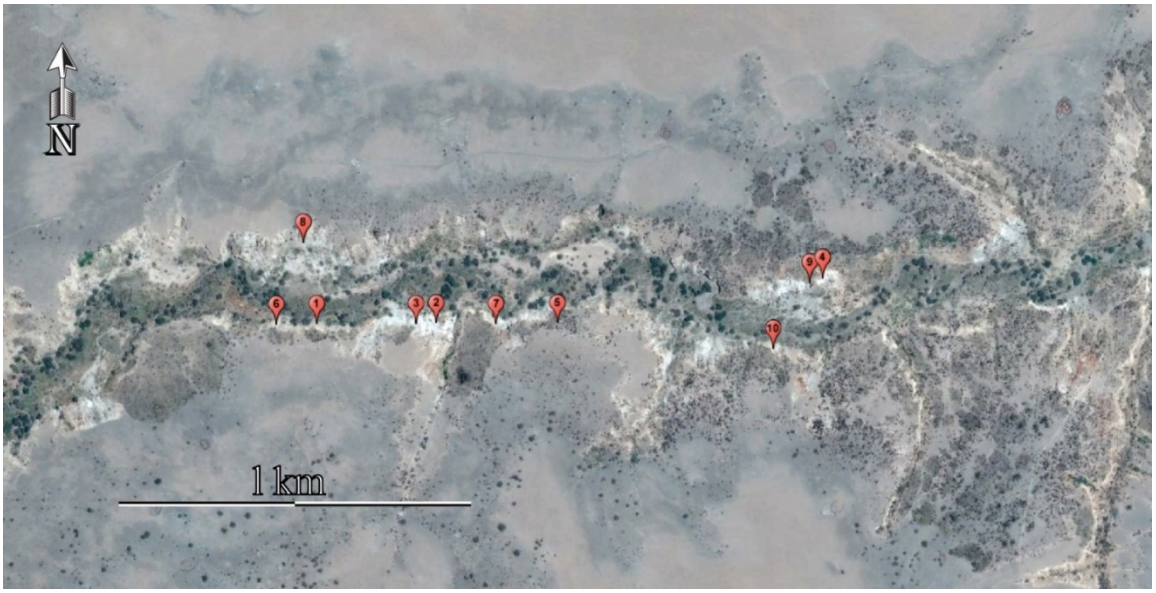

Fig 6: Google Earth map with locations of each of the trenches in the Side Gorge. The number in each bubble corresponds with trench number (i.e. 1=BK-KG-1).

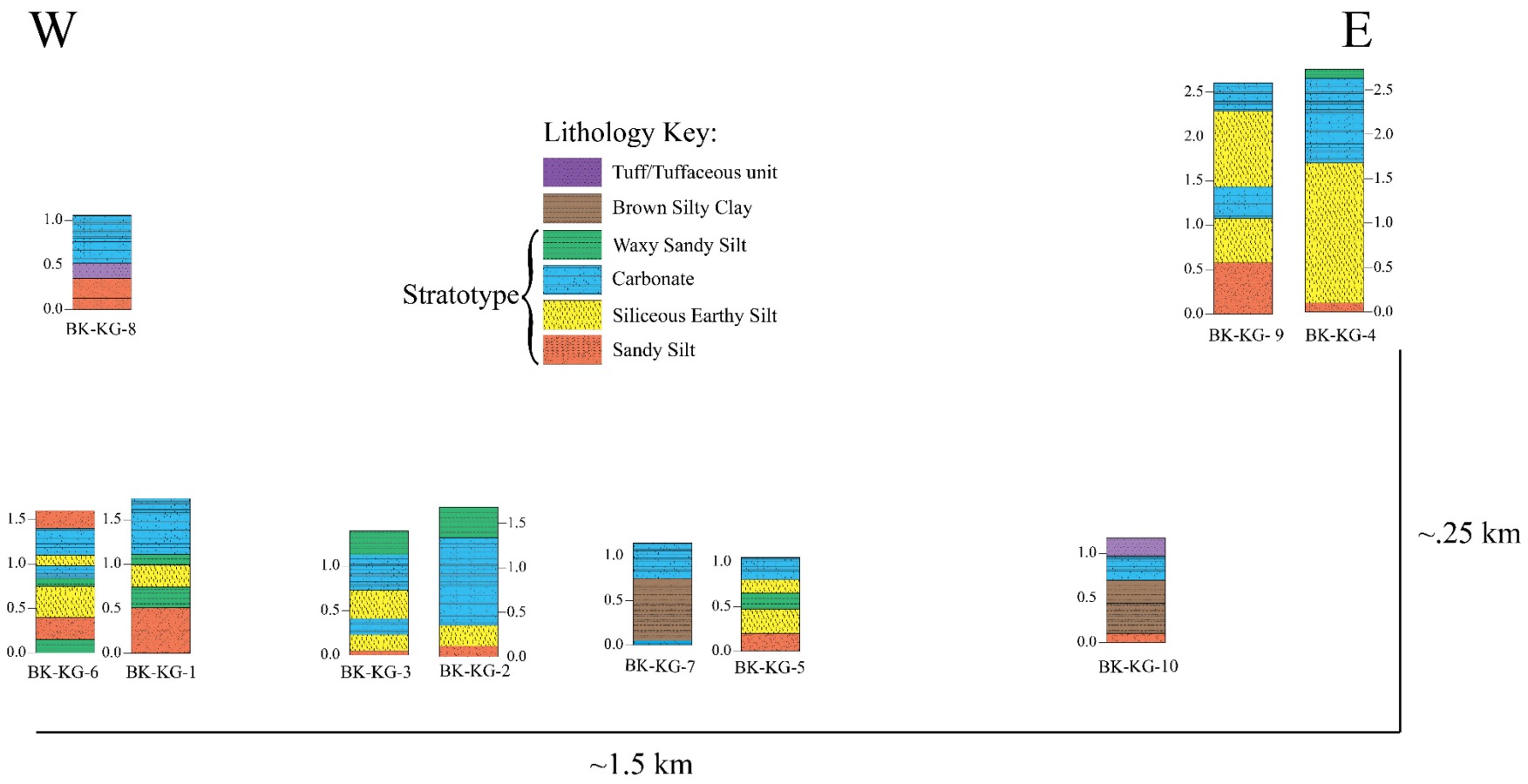

Fig 7: Lithologic Columns of all trenches. Locations correspond to actual positions in the Gorge.

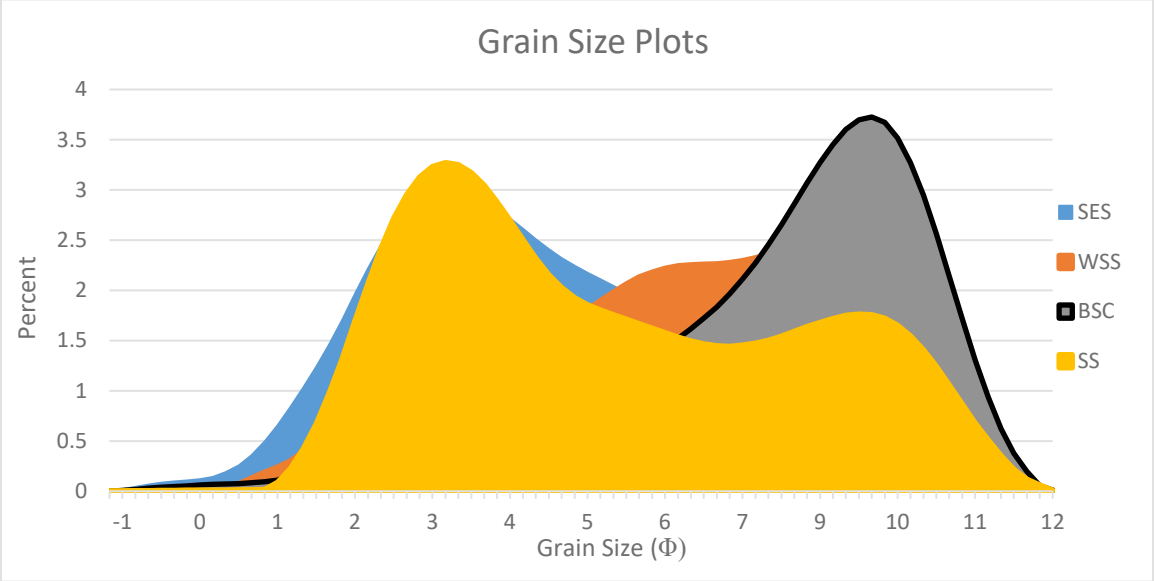

Fig 8: Grain Size curves based on averages for each of the four facies analyzed. SES = siliceous earthy silt. WSS = Waxy Sandy Silt. BSC = Brown Silty Clay. SS = Sandy Silt.

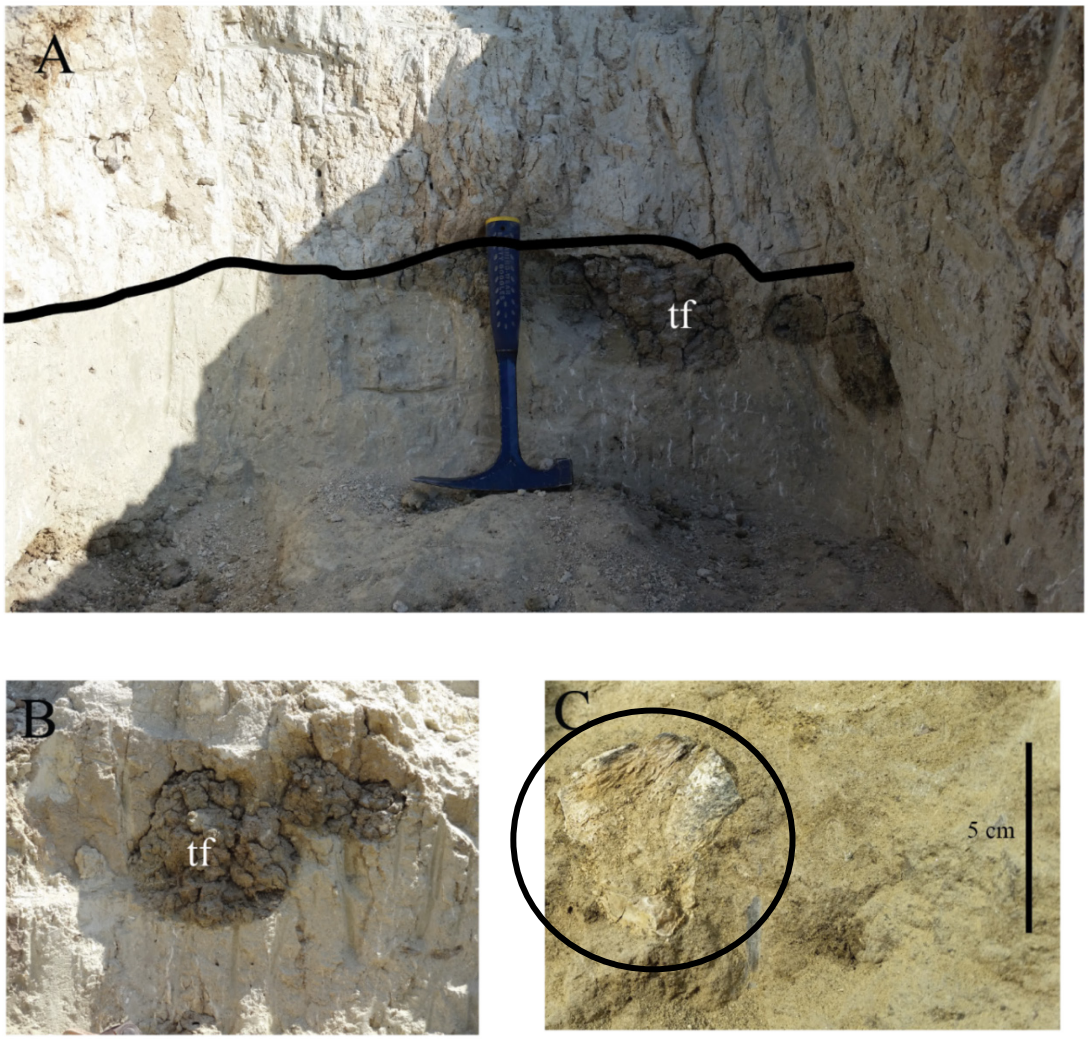

Fig. 9: A) Close up of the siliceous earthy silt in Trench BK-KG-4 at the color boundary. Rhizoliths are more readily seen in the darker lower portion, but are present throughout the photograph. Also present is a potential trace fossil (tf), perhaps a burrow or termatarium which has been infilled with mud. B) Closeup of the same trace fossil from A) at an earlier point in the excavation. C) Detail of the sandstone from Trench BK-KG-1, with an in-situ vertebrate fossil, a proximal tibia, likely from an ungulate (circled).

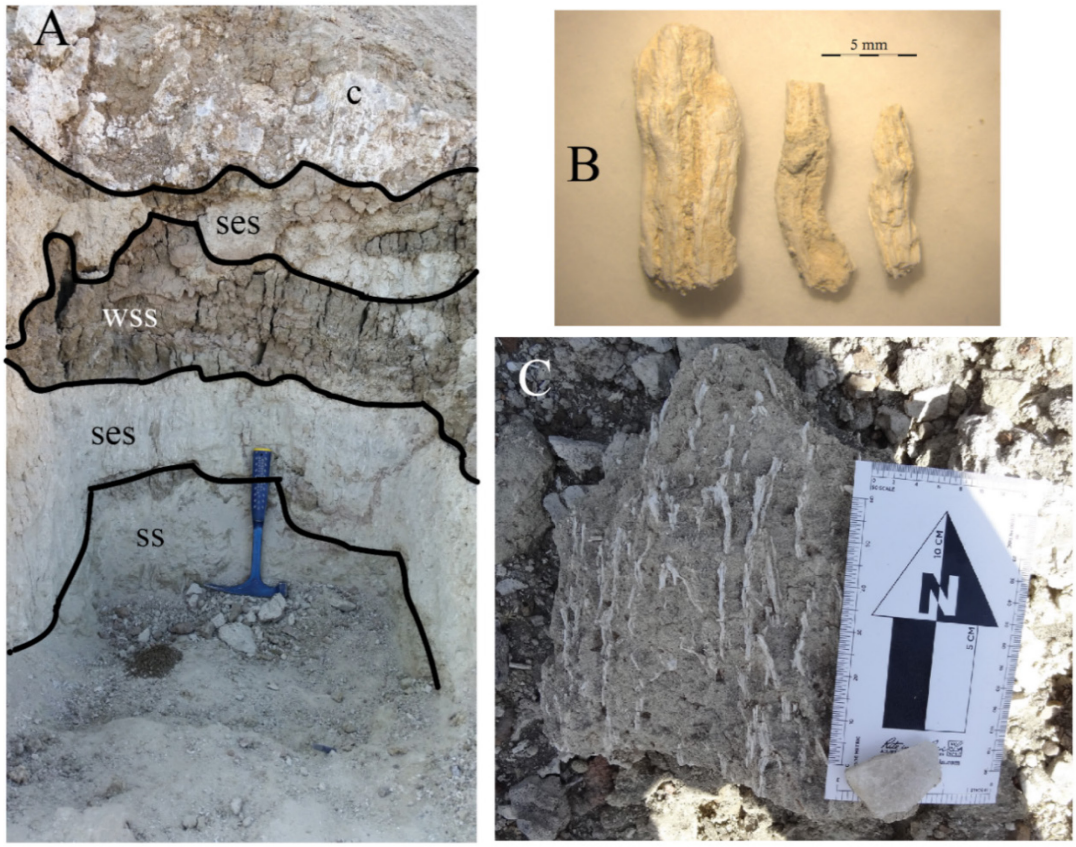

Figure 10: A) Photo of Trench BK-KG-5. From bottom to top are the following facies, separated by solid black lines: ss – sandy silt. ses – siliceous earthy silt. wss –waxy sandy silt. c – carbonate. B) Detail of opaline rhizoliths from the siliceous earthy silt. C) Hand sample of siliceous earthy silt with some of the larger rhizoliths observed near trench BK-KG-4.

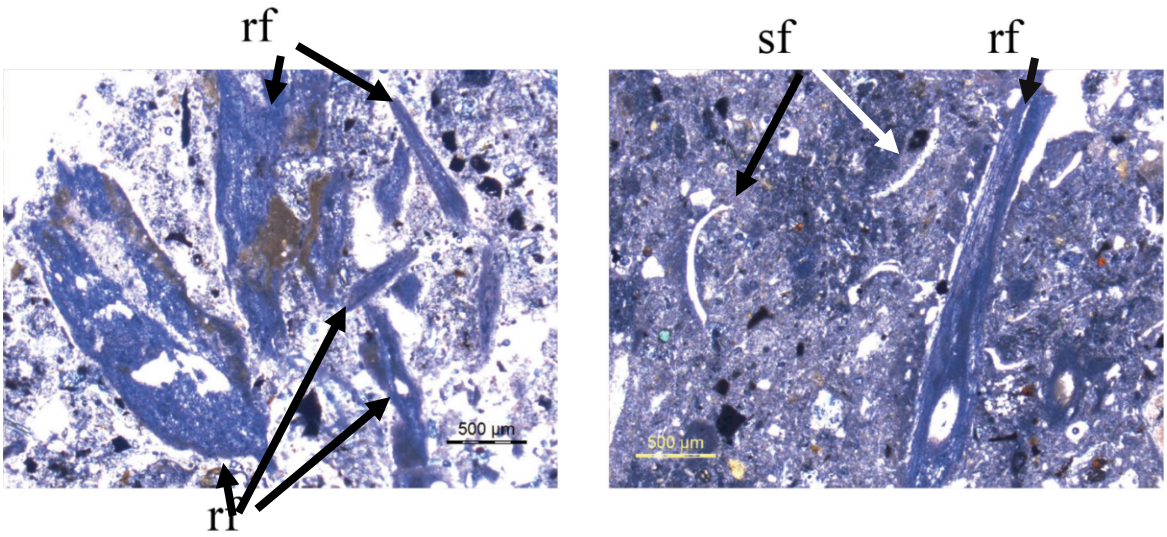

Fig 11: Thin section photomicrographs of the siliceous earthy silt. Fragments of rhizolith composed of Opal-A show are opaque under plane polarized light. rf = rhizolith fragments and sf = shell fragments, most likely from bivalves. Such rhizolith fragments contribute to sand percentage in grain size analysis.

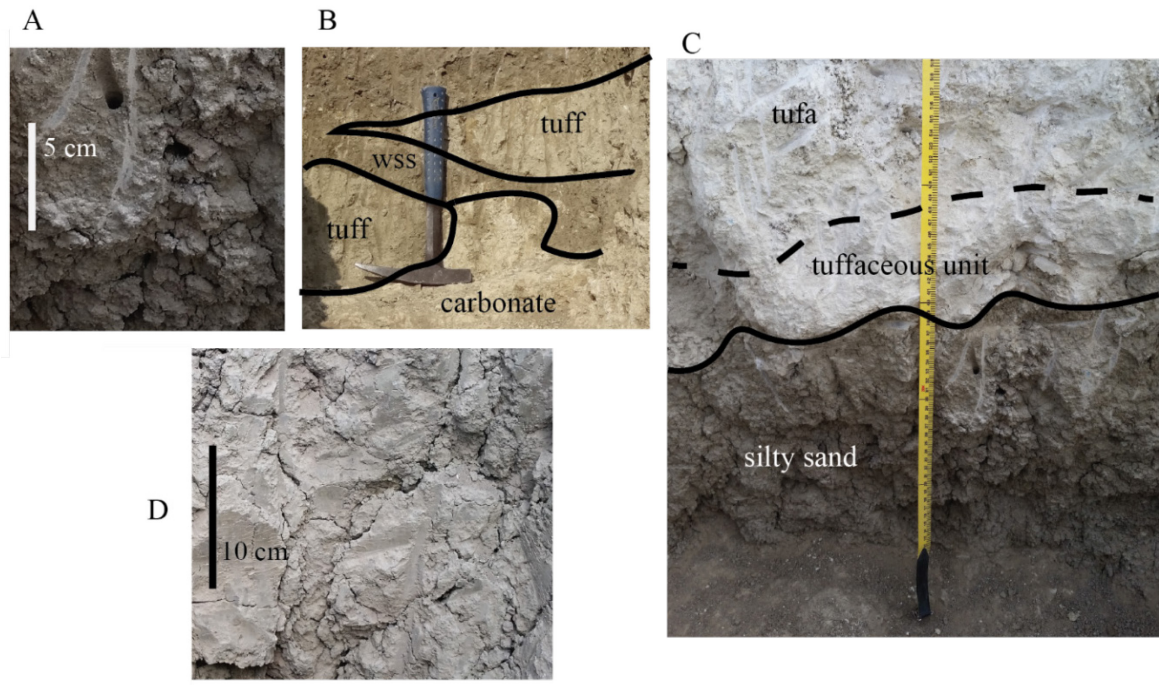

Fig 12: A: Detail of the silty sand facies at as it appears at Trench BK-KG-8. B: Top of trench BK-KG-10, showing a tuff, cut by a waxy silty sand, overlying a carbonate. C: Photo of Trench BK-KG-8. There the silty sand facies has a sharp boundary with the fine tuffaceous unit, which then grades into carbonate. Scale bar = approx. 60 cm. D: Detail of brown silty clay at trench BK-KG-7. Black lines denote facies boundaries.

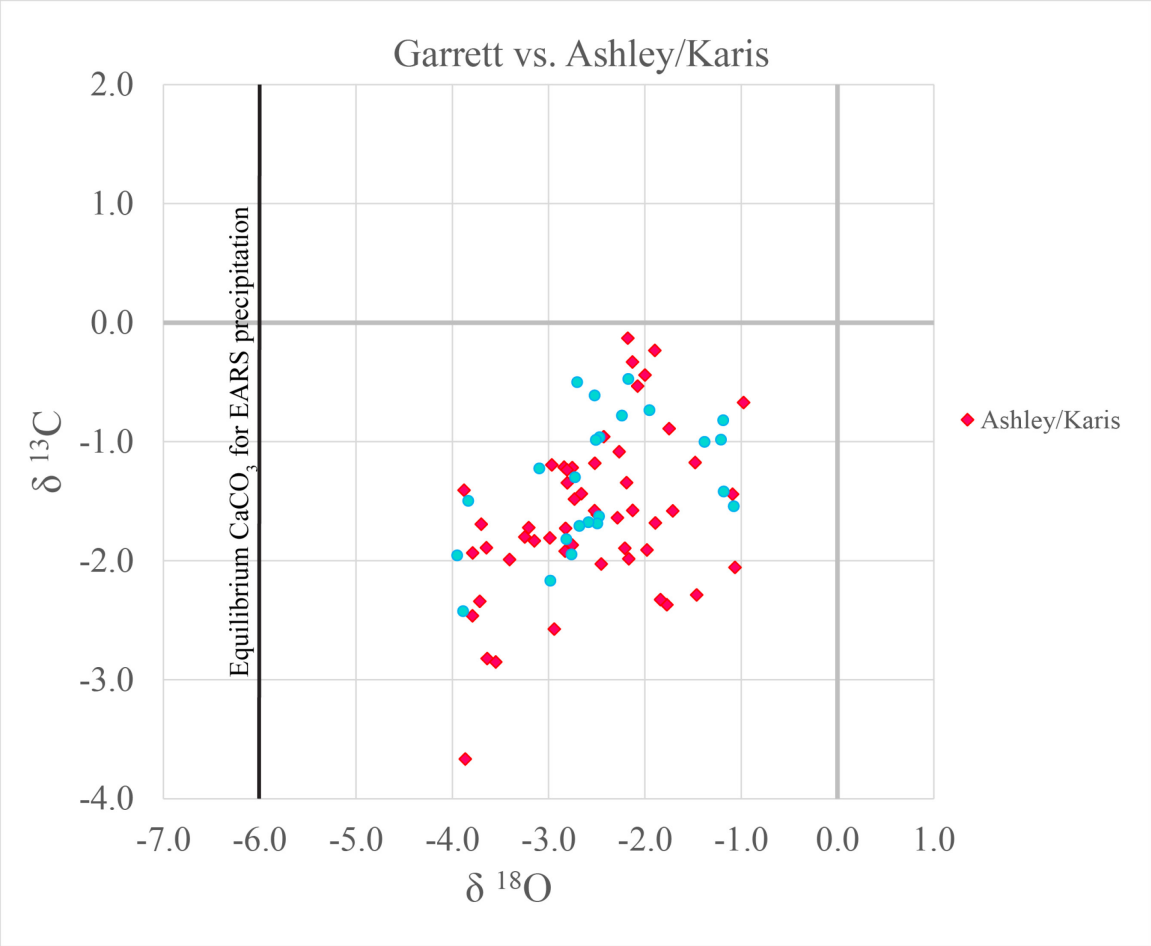

Fig 13: Stable isotope plot comparing data collected for this study (blue) to previously collected samples in red (Karis, 2012; Ashley et al., 2014b). Equilibrium CaCO3 for EARS precipitation denotes the $\delta^{18}O$ value of a carbonate that would precipitate directly from rainfall atop the NVC.

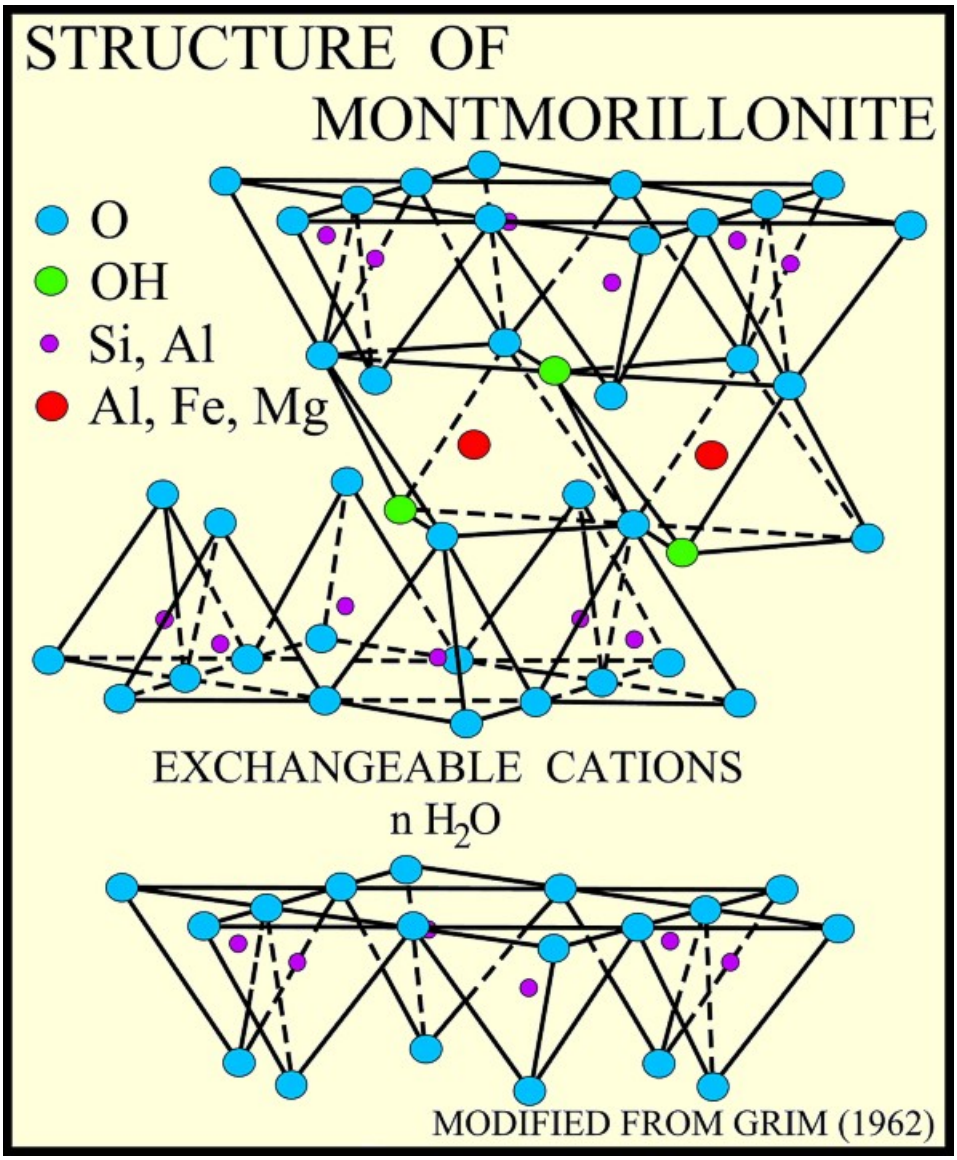

Fig 14: Structure of clay Montmorillonite. Montmorillonite has two tetrahedral layers separated by an octahedral layer, where Al, Fe, or Mg is the octahedral cation. From Poppe et al. (2001).

Facies	Section ID	XRD Bulk Mineralogy	XRD Clay	0-6-0	Octahedral Mg	Q	C	Mg-C	Pg	Z	Px
SES	BK-KG-103	Augite, Pg	Mostly smectite with illite present	1.51250 Å / 61.2328°2θ	1.1						
	BK-KG-203	Pg, Augite, Analclime, Zeolite?(8.44A?)	clay-poor (8.4Aphasepresent)	1.51	1.1						
	BK-KG-305	Calcite, Augite, Pg	Smectite	1.51302 Å / 61.2096°2θ	1.2						
	BK-KG-403	Pg	Smectite	1.50692 Å / 61.4843°2θ	0.7						
	BK-KG-410	Pg	Smectite	1.51196 Å / 61.2571°2θ	1.1						
	BK-KG-509	Augite, Pg	Smectite	1.51042 Å / 61.3263°2θ	1.1						
	BK-KG-606	Pg, Augite	Illite/Smectite	1.51613 Å / 61.0706°2θ	1.6						
	BK-KG-904	Pg, Augite, Analcime, Qtz	clay-poor, some smectite	1.50721 Å / 61.4713°2θ	0.8						
	BK-KG-910	Px, Pg	illite and smectite	1.51199 Å / 61.2556°2θ	1.2						
WSS	BK-KG-107	Phillipsite, Augite	Mostly smectite	1.51418 Å / 61.1575°2θ	1.3						
	BK-KG-109	Pg, Augite, Phillipsite, Analcime, Calcite	Smectite, illite, illite/smectite	1.525Aphase and 1.510Aphase	2/1.1						
	BK-KG-206	Pg, Augite, Analcime, Phillipsite	Illite/Smectite	1.51638 Å / 61.0594°2θ	1.6						
	BK-KG-315	Calcite, Augite, Phillipsite, Pg, Zeolite?(8.4A?)	Illite/Smectite	1.51542 Å / 61.1023°2θ	1.5						
	BK-KG-508	Px, Chabazite, Pg	Illite/Smectite	1.51006 Å / 61.3423°2θ	1.1						
	BK-KG-601	Mg-c, Pg, Qtz, Analcime, Zeolite?(8.4A?)	Illite/Smectite	1.51509 Å / 61.1171°2θ	1.5						
	BK-KG-607	Mg-c, Augite, Chabazite	Illite/Smectite	1.51324 Å / 61.1998°2θ	1.2						
BSC	BK-KG-703	Pg, Augite, Analcime, Chabazite(tr), Qtz	Illite	1.51288 Å / 61.2160°2θ	1.2						
	BK-KG-705	Pg, Augite, Analcime, Chabazite(tr), Qtz	Illite	1.51227 Å / 61.2434°2θ	1.1						
	BK-KG-1001	Analcime, chabazite, Pg	Illite	1.50971 Å / 61.3585°2θ	0.9						
	BK-KG-1010	Analcime, chabazite, Pg	Illite	1.51	1.1						

Fig. 15: Clay mineral results table. SES = Siliceous Earthy silt. WSS = Waxy sandy silt. BSC = brown silty clay. Q = quartz, C = calcite, Mg-C = Magnesium calcite, Pg = plagioclase, Z = zeolite, Px = Pyroxene. Octahedral Mg values inferred

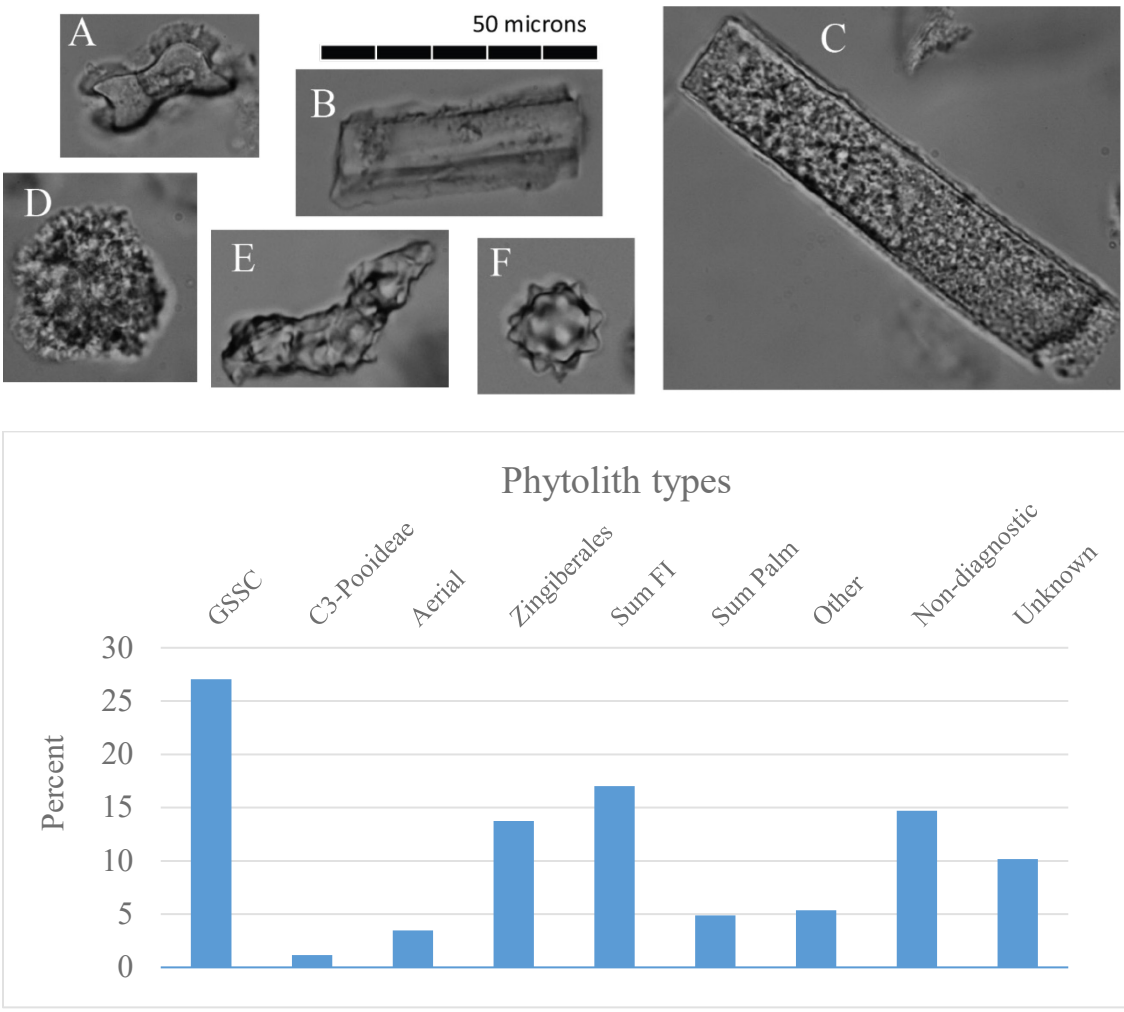

Fig 16: Phytoliths from the BK wetland. A: bilobate C4 grass phytolith. B: Crenate Pooidae C3 cell from a high elevation grass. C: Rectangular plate-like body from an aerating root system. D: Globular rugulose granulate from order Zingiberales.. E: Ellipsoid echinate from *Boscia senegalensis*, a forest indicator F: Globular echinate from a palm (Arecaceae). Photos by Doris Barboni. Scale applies to all photos. Below: Bar graphs representing the percentages of the phytolith assemblage from the study.

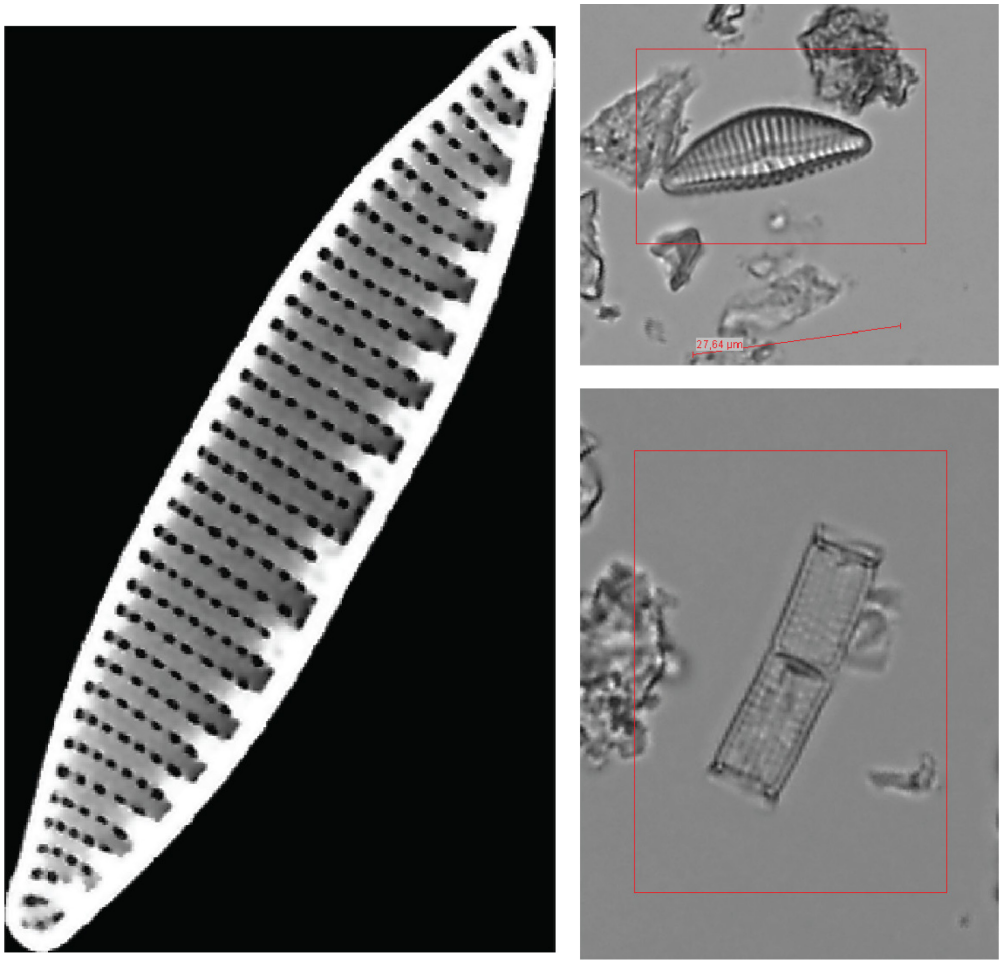

Fig. 17: Left: Image of *Nitschia amphibia* courtesy R. Bernhart Owen. Top Right: Image of *Encyonema silesiacum* from samples of siliceous earthy silt previously collected. Bottom Right: *Aulacoseira granulata* from the same samples. Right images courtesy Hector Arraiz.

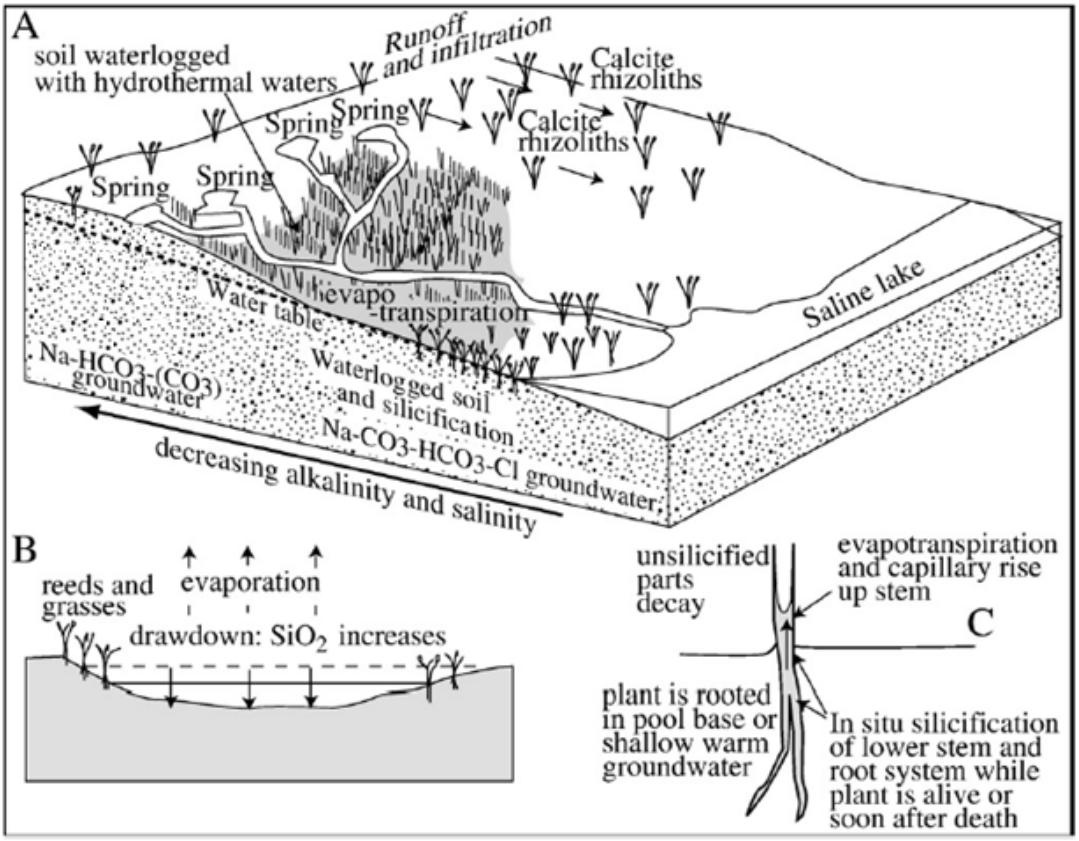

Fig. 18: Schematic of silicate rhizolith formation in an environment similar to the BK wetland. Evapotranspiration and capillary forces draw Si-rich water through plants even after death, where cellular material is replaced with amorphous Si. Modified from Owen et al. (2009).

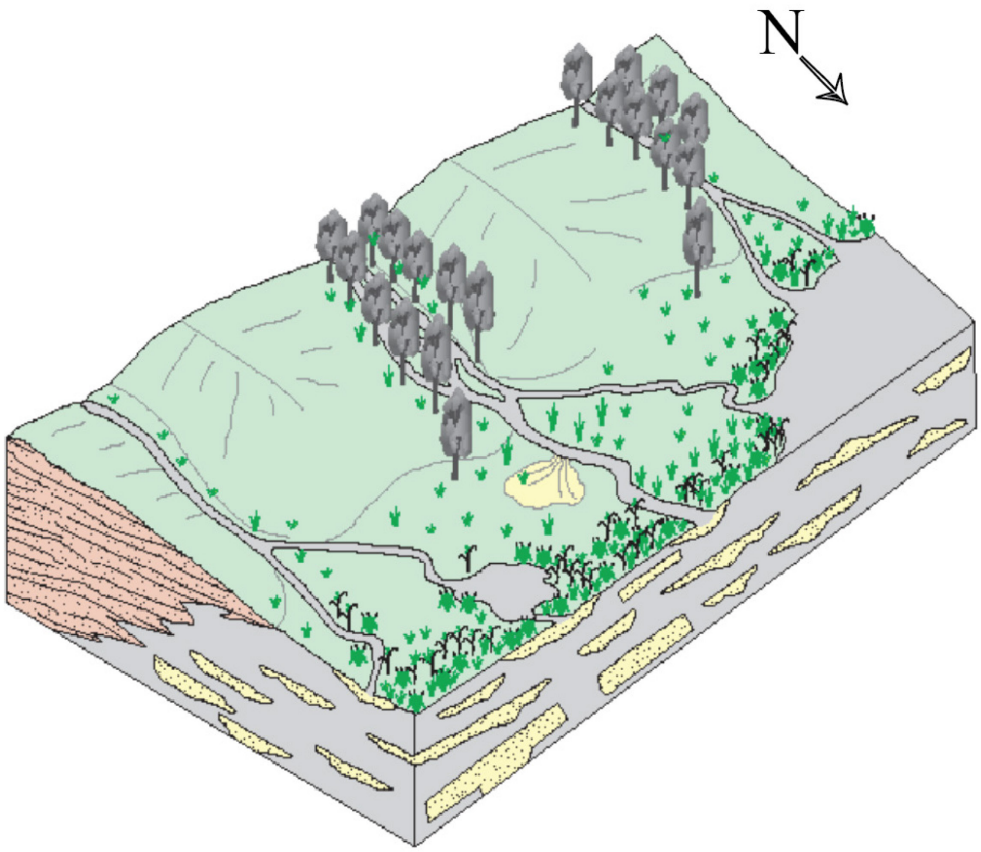

Fig 19: Cartoon of proposed paleoenvironmental reconstruction. Delta distributaries interfinger among wetlands fringing a lake. This system sits atop sandy lake margin deposits, Relict distributary deposits are seen in cross section. Modified from Arenas et al. (2007).

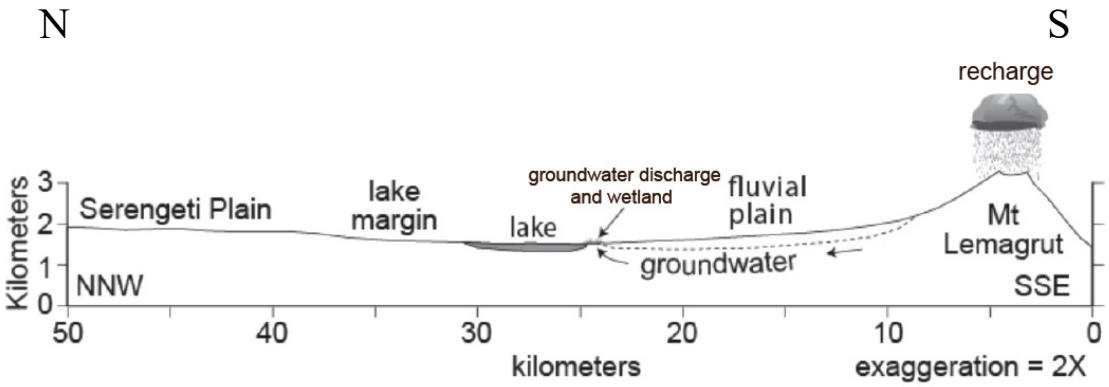

Fig 20: Cartoon illustrating the groundwater flow from Lemagurut to the Olduvai Basin. Freshwater crops out near the saline lake at the center of the basin.

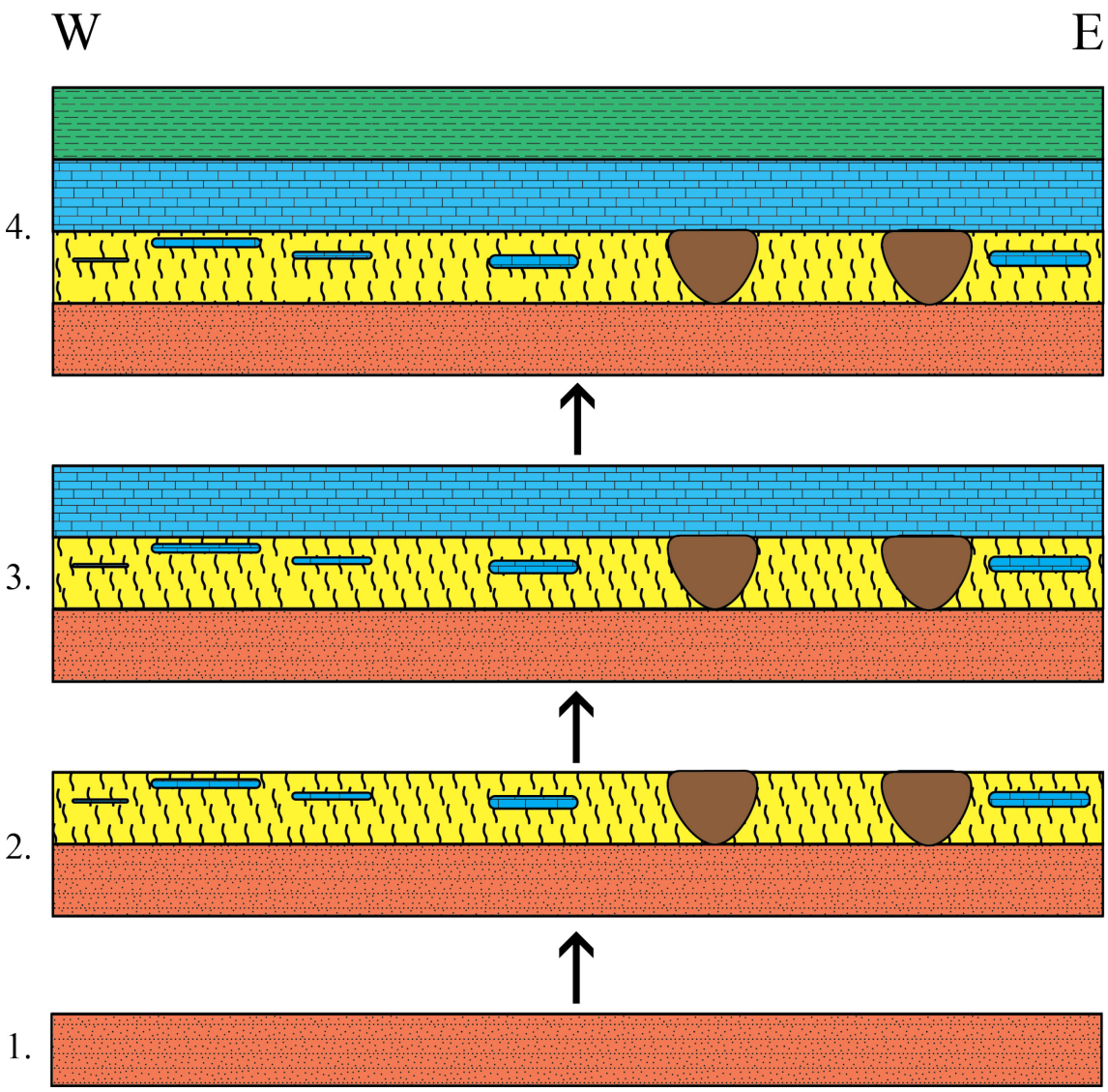

Fig. 21: Schematic of the facies succession as the environment changes over time. Time 1: Littoral sand/terminal sandy splays (orange) are widespread. Time 2: The landscape is largely siliceous earthy silt (yellow). Some carbonate-precipitating pools are present (blue), but are limited in space and time. Channels are cut, which are later filled with brown silty clay (brown). Time 3: Carbonate dominates the landscape and is precipitated in a continuous tufa bed (blue). Paleo Lake Olduvai transgresses the landscape and waxy sandy silts (green) are deposited.

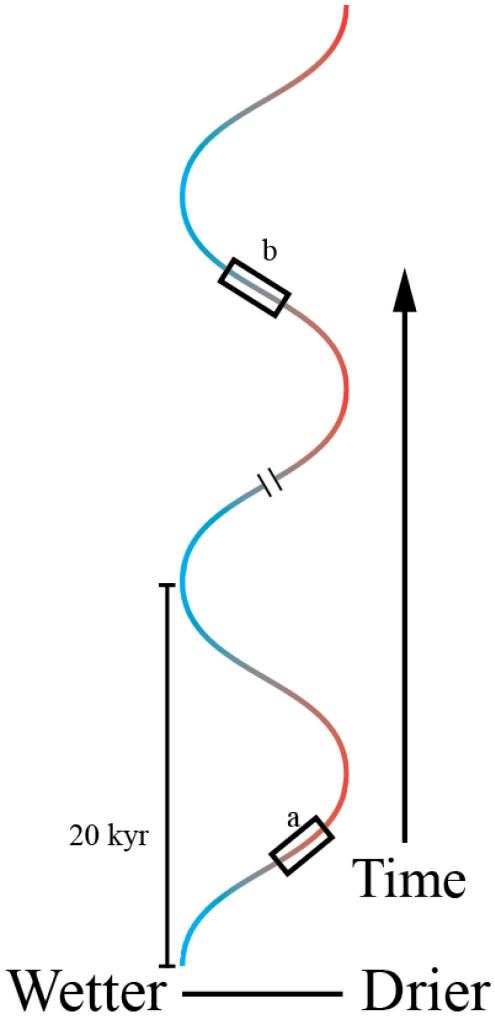

Fig. 22: Relative positions of Olduvai tufas on a precession scale. Most observed tufas occur in position a: on the waning limb of a precession cycle, where precipitation from the preceding maximum moves through the groundwater system from the NVC to the Olduvai basin. Position b represents the tufa described here, which occurs on the waxing limb of a precession cycle.

APPENDICES

APPENDIX I.

GPS coordinates for trenches

GPS coordinates	
Trench BK-KG-1	02°59.765'S 035°19.343'E
Trench BK-KG-2	02°59.764'S 035°19.527'E
Trench BK-KG-3	02°59.765'S 035°19.496'E
Trench BK-KG-4	02°59.694'S 035°20.123'E
Trench BK-KG-5	02°59.764'S 035°19.714'E
Trench BK-KG-6	02°59.766'S 035°19.281'E
Trench BK-KG-7	02°59.765'S 035°19.619'E
Trench BK-KG-8	02°59.640's 035°19.323'E
Trench BK-KG-9	02°59.701'S 035°20.103'E
Trench BK-KG-10	02°59.803'S 035°20.048'E

APPENDIX II.

Grain Size Data

Sample	Trench	Height (cm)	Mean φ	Sorting φ	Skewness
BK-KG-101	BK-KG-1	75	4.922	2.092	0.757
BK-KG-104	BK-KG-1	90	4.868	2.134	0.431
BK-KG-106	BK-KG-1	100	4.058	2.081	0.868
BK-KG-109	BK-KG-1	60	5.547	2.894	0.021
BK-KG-201	BK-KG-2	17.5	4.703	2.942	0.432
BK-KG-202	BK-KG-2	25	6.749	2.901	-0.327
BK-KG-203	BK-KG-2	30	5.605	2.517	-0.204
BK-KG-204	BK-KG-2	35	7.131	2.449	-1.130
BK-KG-206	BK-KG-2	165	6.303	2.540	-0.144
BK-KG-207	BK-KG-2	10	8.132	1.885	-1.305
BK-KG-301	BK-KG-3	5	2.779	1.954	1.198
BK-KG-303	BK-KG-3	15	4.081	2.303	0.674
BK-KG-306	BK-KG-3	50	4.330	2.091	0.364
BK-KG-309	BK-KG-3	65	7.031	2.336	-0.694
BK-KG-310	BK-KG-3	70	4.367	2.685	0.423
BK-KG-315	BK-KG-3	120	5.786	2.540	0.138
BK-KG-316	BK-KG-3	0	5.025	2.799	0.410
BK-KG-401	BK-KG-4	10	3.799	2.058	1.030
BK-KG-404	BK-KG-4	55	5.386	2.230	0.106
BK-KG-406	BK-KG-4	85	6.220	2.002	-0.439
BK-KG-409	BK-KG-4	130	5.520	2.237	-0.030
BK-KG-410	BK-KG-4	145	5.182	2.330	0.200
BK-KG-413	BK-KG-4	265	6.170	2.631	-0.115
BK-KG-414	BK-KG-4	5	3.991	1.897	1.107
BK-KG-501	BK-KG-5	5	5.544	2.405	0.565
BK-KG-505	BK-KG-5	20	3.599	2.116	1.099
BK-KG-507	BK-KG-5	45	3.961	2.189	0.712
BK-KG-508	BK-KG-5	55	6.697	2.129	-0.133
BK-KG-509	BK-KG-5	75	4.688	1.937	0.677
BK-KG-601	BK-KG-6	10	4.056	2.694	1.037
BK-KG-602	BK-KG-6	20	3.684	1.891	1.401
BK-KG-604	BK-KG-6	50	4.570	2.455	0.572
BK-KG-606	BK-KG-6	70	3.507	2.368	0.764

BK-KG-607	BK-KG-6	80	6.894	2.535	-0.551
BK-KG-610	BK-KG-6	105	6.447	2.410	-0.074
BK-KG-613	BK-KG-6	145	6.172	2.388	0.253
BK-KG-701	BK-KG-7	10	7.065	2.280	-0.327
BK-KG-702	BK-KG-7	20	7.269	2.574	-0.800
BK-KG-703	BK-KG-7	30	6.591	2.817	-0.311
BK-KG-705	BK-KG-7	50	4.292	2.591	1.036
BK-KG-706	BK-KG-7	60	5.855	2.935	-0.028
BK-KG-707	BK-KG-7	70	7.200	2.442	-0.964
BK-KG-801	BK-KG-8	5	7.472	2.597	-0.905
BK-KG-803	BK-KG-8	20	5.546	2.883	0.239
BK-KG-804	BK-KG-8	27.5	6.599	2.904	-0.768
BK-KG-903	BK-KG-9	75	4.434	2.071	0.130
BK-KG-905	BK-KG-9	105	5.326	2.484	-0.229
BK-KG-907	BK-KG-9	155	5.066	2.434	0.159
BK-KG-910	BK-KG-9	200	5.387	2.028	0.366
BK-KG-912	BK-KG-9	230	3.439	2.370	1.101
BK-KG-1001	BK-KG-10	5	8.689	1.280	-0.876
BK-KG-1003	BK-KG-10	15	7.874	1.778	-0.774
BK-KG-1006	BK-KG-10	30	7.350	2.441	-1.018
BK-KG-1008	BK-KG-10	40	6.881	2.557	-0.341
BK-KG-1010	BK-KG-10	50	6.611	3.015	-0.614
BK-KG-1012	BK-KG-10	60	6.790	3.010	-0.412

APPENDIX III.

Stable C and O isotope data

Sample ID	δC^{13} PDB	δO^{18} PDB	RU#	Trench
BK-KG-110	-0.50	-2.70	20160157	BK-KG-1
BK-KG-205	-0.47	-2.17	20160146	BK-KG-2
BK-KG-311	-1.22	-3.10	20160153	BK-KG-3
BK-KG-312	-0.98	-2.51	20160137	BK-KG-3
BK-KG-313	-1.68	-2.59	20160149	BK-KG-3
BK-KG-314	-1.30	-2.73	20160152	BK-KG-3
BK-KG-412	-0.73	-1.95	20160148	BK-KG-4
BK-KG-510	-1.63	-2.48	20160134	BK-KG-5
BK-KG-605	-0.61	-2.52	20160142	BK-KG-6
BK-KG-608	-0.78	-2.24	20160141	BK-KG-6
BK-KG-611	-1.71	-2.68	20160140	BK-KG-6
BK-KG-612	-1.82	-2.82	20160150	BK-KG-6
BK-KG-708	-0.96	-2.47	20160138	BK-KG-7
GA-27-15	-1.00	-1.38	20160139	BK-KG-8
GA-28-15	-0.98	-1.21	20160143	BK-KG-8
GA-29-15	-0.82	-1.19	20160136	BK-KG-8
GA-30-15	-1.54	-1.08	20160132	BK-KG-8
GA-31-15	-1.42	-1.18	20160151	BK-KG-8
GA-32-15	-1.69	-2.49	20160154	BK-KG-8
BK-KG-906	-2.17	-2.98	20160133	BK-KG-9
BK-KG-913	-1.95	-2.76	20160156	BK-KG-9
BK-KG-1014	-2.42	-3.89	20160147	BK-KG-10
GA-33-15	-1.50	-3.84	20160135	BK-KG-10
GA-34-15	-1.96	-3.95	20160155	BK-KG-10

Sample	Height	Phyto lab#	status	GSSC %	C3-Pooideae %	Fan shaped %	Sedges %	Aerial %	Zingiberales	Sum FI %	Sum Palm %	Non-diagnostic %	Unknown %
BK-KG-102	0.80 m	88/1	good	14.3	3.5	14.8	2.8	2.3	6.8	20.3	2.3	24.3	12.0
BK-KG-202	0.25 m	88/2	good	38.8	0.0	1.2	0.0	6.5	17.1	15.4	0.0	13.0	5.8
BK-KG-204	0.35 m	88/3	*slide to be redone*	-	-	-	-	-	-	-	-	-	-
BK-KG-106	1.0 m	88/4	good	22.4	1.1	6.9	0.0	8.6	5.6	14.8	0.7	16.0	15.2
BK-KG-301	0.10 m	88/5	good	21.4	0.0	4.4	0.0	11.5	9.0	23.4	0.2	17.8	9.8
BK-KG-308	0.60 m	88/6	*slide to be redone*	-	-	-	-	-	-	-	-	-	-
BK-KG-402	0.25 m	88/7	*Good*	27.1	0.0	1.0	0.0	2.1	7.3	21.9	0.0	16.7	13.5
BK-KG-408	1.15 m	88/8	excellent	33.9	0.0	3.0	3.7	0.0	2.1	11.3	26.2	11.7	3.9
BK-KG-503	0.25 m	89/1	good	13.9	0.0	0.8	0.0	0.7	59.3	5.5	0.0	3.7	13.6
BK-KG-508	0.60 m	89/2	excellent	33.2	0.0	9.7	1.0	1.5	5.1	14.3	1.0	22.7	8.9
BK-KG-604	0.50 m	89/3	good	37.5	0.0	0.0	0.0	3.1	26.6	15.6	0.0	4.7	9.4
BK-KG-609	1.0 m	89/4	*sterile*	*sterile*									
BK-KG-903	0.75 m	89/5	excellent	25.5	0.0	3.7	0.0	1.3	8.3	15.6	23.2	15.2	6.0
BK-KG-912	2.3 m	89/6	excellent	29.6	8.0	5.9	0.2	0.5	4.0	29.0	0.0	15.8	13.6

Appendix IV.

Phytolith Data

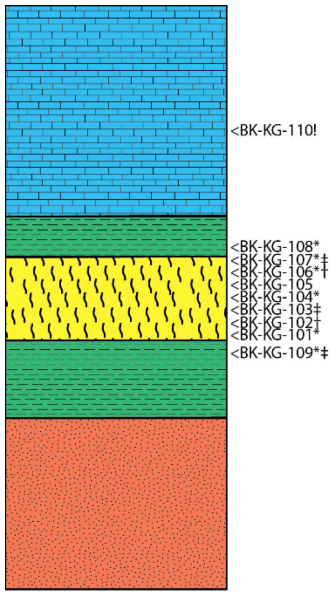

BK-KG-1

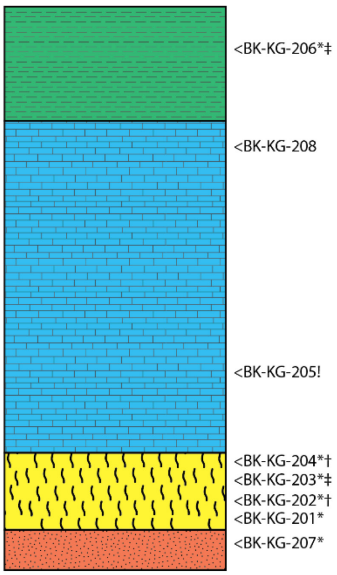

BK-KG-2

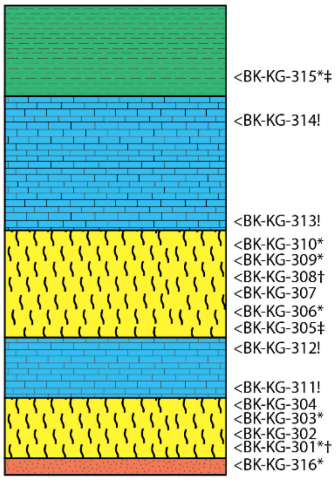

BK-KG-3

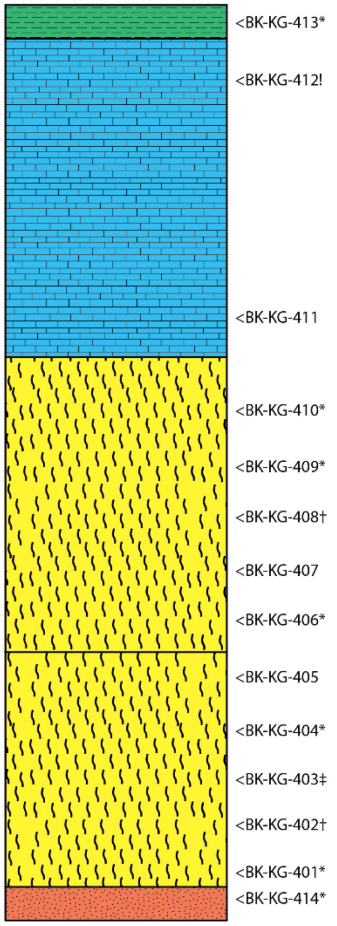

BK-KG-4

Appendix V.

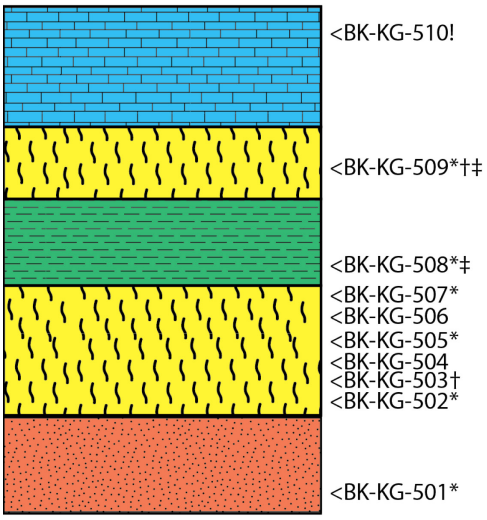

BK-KG-5

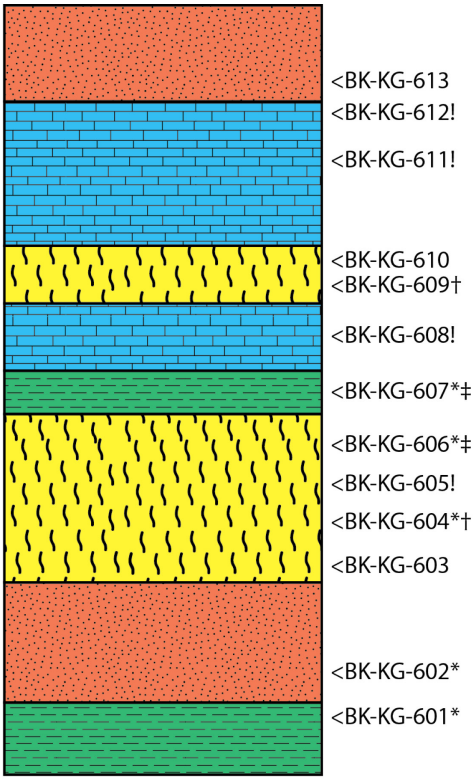

BK-KG-6

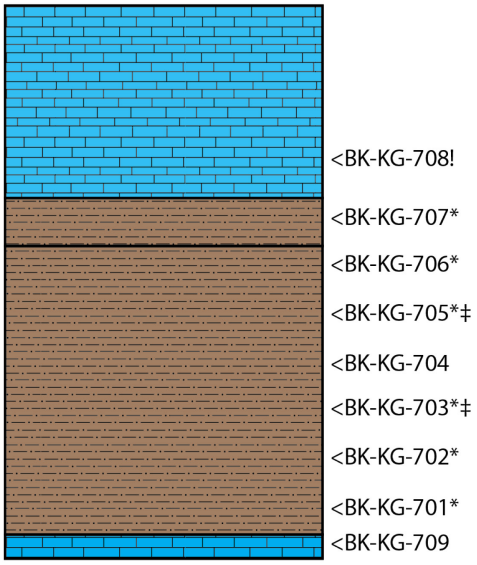

BK-KG-7

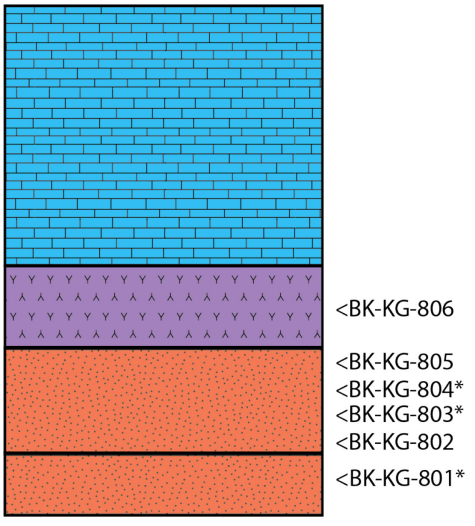

BK-KG-8

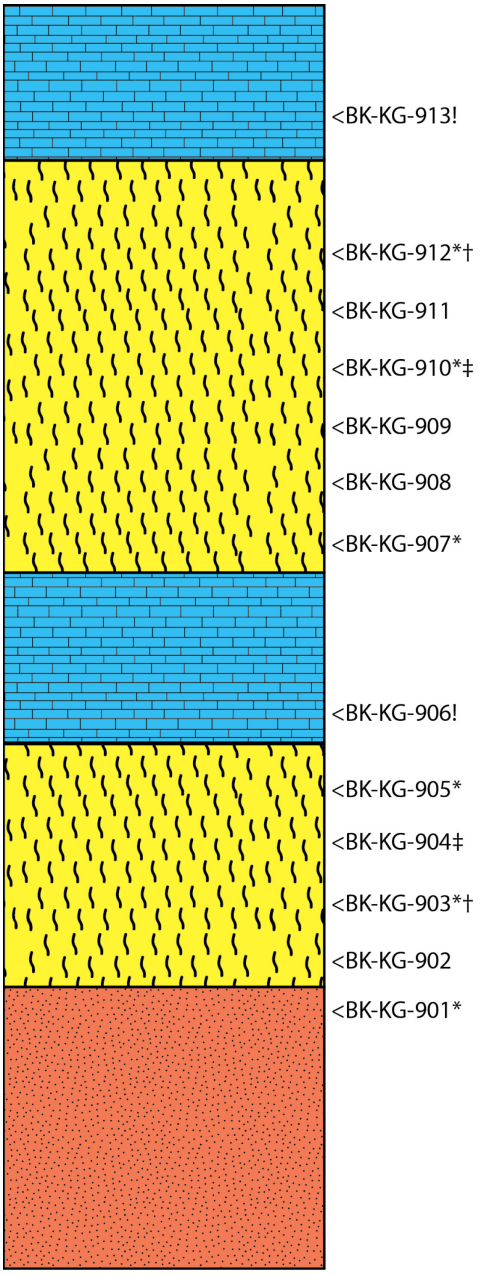

BK-KG- 9

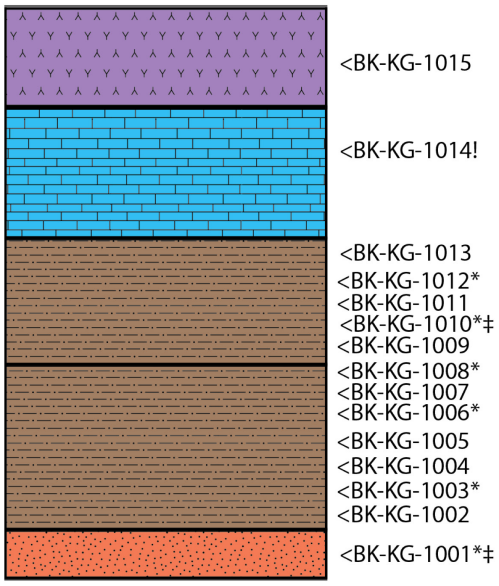

BK-KG-10

Key: * = grain size analysis

! = Stable isotope analysis

† = Diatom/phytolith analysis

‡ = XRD analysis

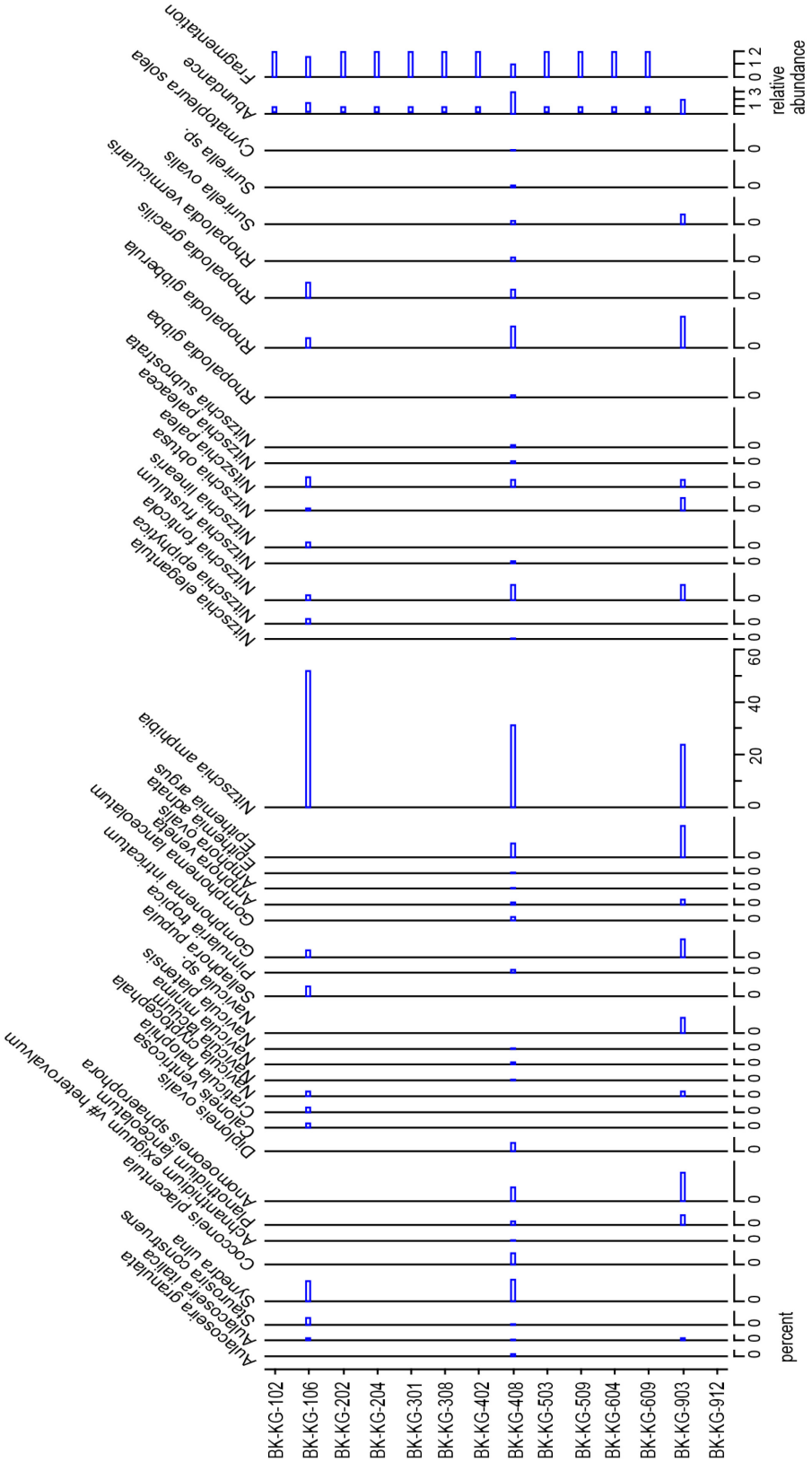

Appendix VI.

Diatom data